All-Optical Switching and Variable Delay Using Nonlinear Optical Signal Processing Techniques

CHENG, Lap Kei

A Thesis Submitted in Partial Fulfillment
of the Requirements for the Degree of
Master of Philosophy
in
Electronic Engineering

September 2008

Abstract of thesis entitled:
All-Optical Switching and Variable Delay Using Nonlinear Optical Signal Processing Techniques
Submitted by Cheng Lap Kei
for the degree of Master of Philosophy in Electronic Engineering
at The Chinese University of Hong Kong in July 2008.

Abstract

Variable delay and switching circuit are the fundamental building blocks in an optical communication network. The optical fiber offers virtually unlimited transmission bandwidth, thus supporting a great increase in the data transmission rate over the last decade. However, optical to electrical conversion is required in switching or in delaying the communication data. The channel bit-rate is thus limited by the speed of available electronic components and circuits. Owing to the ultrafast response of nonlinear optical phenomena, all-optical switch and all-optical delay line can be used to replace the existing optical to electrical conversion and supports high bit-rate communication.

In this research thesis, all-optical switching of 10 Gb/s differential-phase-shift keying (DPSK) signal is demonstrated in an semiconductor optical amplifier (SOA) using nonlinear polarization rotation (NPR). The phase information and the signal wavelength are preserved throughout the switching processes. Optical variable delay line, together with all-optical switching, can serve as a buffer. Variable delay time can be achieved using slow light via stimulated Brillouin scattering. However, the technique has a limited operating bandwidth. It also requires precise alignment between the signal wavelength and the SBS induced resonance to achieve a large delay. A solution to increase the operating bandwidth is demonstrated using a phase-modulated pump. The gain bandwidth of SBS slow light is enhanced to delay

a 26 ps optical pulse by 10 ps using the pump source. Owing to the constant intensity of a phase-modulated pump, no synchronization is needed between the pump and the signal pulses. Hence, the approach offers a practical means in delaying true optical data. We also design a slow light system independent of the signal wavelength. The design eliminates the need of precise tuning of the pump wavelength in SBS slow light technique. By using a wavelength converter and a fiber Brillouin laser, automatic alignment with the SBS induced resonance is achieved regardless of the input signal wavelength. The maximum delay achieved is 26 ns for a 30 ns optical pulse. The delay variation is less than 0.2 ns over 40-nm signal wavelength detuning.

Apart from slow light techniques, tunable delay can be achieved with wavelength conversion together with group velocity dispersion. A fast channel selectable demultiplexing on a 40-Gb/s OTDM signal is demonstrated using FWM wavelength conversion and group velocity dispersion in a chirped fiber Bragg grating. We also demonstrate tunable delay with CSRZ-OOK to RZ-OOK data format conversion using pump modulated FWM. The maximum delay achieved is 200 ps. No power penalty is obtained in the receiver sensitivity at a BER of 10^{-9}. The scheme offers a simple solution to delay and convert CSRZ data to RZ data in high speed optical communication network.

摘要

可變時延器件和光開關是光纖通訊網絡中的基礎組件。在過去十年，即使數據傳輸率一再提升，光纖依然能夠支持。它的傳輸帶寬可認爲幾乎沒有限制。然而，採用光電轉換方式的時延器件和開關卻因爲現有電子器件和線路的處理速度不夠而限制了信道的比特率。由於非線性光學效應的響應速度非常快，全光開關和全光延遲線可以替代傳統的光電轉換方式，支持更高的比特率。這是研究這兩個全光器件的主要原因。

本論文首先展示了一個用於 10-Gb/s 差分相位鍵移(DPSK)信號的全光開關，利用了半導體光放大器(SOA)的非線性偏振旋轉。信號的相位信息和波長都沒有被改變。除了全光開關,光緩存器還需要一個全光可變延遲線。可變時延可以通過受激布裡淵散射(SBS)形成慢光來實現.通常的方案有兩個缺點，一是工作帶寬窄，二是信號波長和 SBS 諧振波長需要精確對准才能產生較大的時延。我們使用相位經過調制的 SBS 泵浦解決了第一個缺。SBS 慢光的增益帶寬得到加寬,並使得一個 26 ps 寬的脈沖被延遲了 10 ps。由於泵浦隻是相位被調制過，光強仍然恆定，所以不存在泵浦和信號之間的同步問題，使得這個方案適用於實際的光信號。我們也設計出了一個獨立於信號波長的 SBS 慢光系統，使之對不同的信號波長都不需要調節泵浦波長。這裡面用到了波長轉換和一個光纖布裡淵激光器，自動完成信號波長與 SBS 諧振的對准。系統把一個 30 ns 寬的光脈沖最大延遲了 26 ns，並且在信號波長變動超過 40 nm 的范圍內，時延差異小於 0.2 ns。

除了慢光,波長轉換結合群速度色散（GVD）也可以實現可變延遲。利用四波混頻（FWM）作波長轉換和啁啾布拉格光纖光柵（CFBG）提供的 GVD，我

們實現了對 40-Gb/s 光時分復用信號的解復用,可以選擇性地解調出不同的子信道。此外，利用以光信號作爲泵浦的 FWM,在實現最高達到 200 ps 時延的同時，我們還做到了 CSRZ-OOK 到 RZ-OOK 數據格式的轉換。並且在誤碼率爲 10^{-9} 的水平上，沒有功率損失。這個方案在高速光通訊網絡中同時簡易地實現了數據延遲和 CSRZ 到 RZ 格式的轉換兩個功能。

Acknowledgements

I would like to thank those who have helped me to complete my research for my master degree. First and for most, I have to express my deep gratitude to my supervisor, Prof. Chester Shu, for his continuous support, guidance and kindness throughout the course of my research study. His ideas and insights on fiber optics technology enlarged my knowledge base in the field. I would also like to dedicate this work to my parents and my sister and brother for their support and encouragement.

I would like to express my appreciation and thankfulness to Dr. Mable P. Fok for training me to be familiarized with the equipment in laboratory. I would also like to thank for her continuous support, discussion and encouragement. I am also grateful to Barbara L. C. Ho for her technical assistances and support in the optoelectronics laboratory.

I would like to thank Prof. H. K. Tsang and Prof. K. T. Chan for raising my interest on photonics through their classes.

I would like to express my appreciation to my colleagues Mr. K. P. Lei, Mr. Y. H. Dai, Mr. L. Xu, Mr. X. Chen, and Mr. C. Y. Wong, Mr. K. J. Chen, Mr. H. Hao, Mr. Y. Tao, Mr. Z. X. Zhang, and Ms. M. Y. Chen. Also thank Mr. Y. H. Dai for helping me in translating the thesis abstract to Chinese.

Table of contents

ABSTRACT I

摘要 III

ACKNOWLEDGEMENTS V

TABLE OF CONTENTS IV

INTRODUCTION 0

1.1 Different ways to achieve all-optical tunable delay 2

1.1.1 Optical buffer realized with optical switching 2

1.1.2 Slow light technique 3

(i) Basics of slow light 4

(ii) Slow light via electromagnetically induced transparency (EIT) 6

(iii) Slow light via coherent population oscillation (CPO) 7

(iv) Slow light via optical parametric amplification(OPA) 8

(v) Slow light via stimulated Raman and Brillouin scattering 8

1.1.3 Tunable delay using wavelength conversion together with chromatic dispersion 10

1.1.4 Comparison of different schemes for constructing all-optical delay line 11

1.2 Overview of the thesis 12

References 14

ALL-OPTICAL SWITCHING OF DPSK SIGNAL IN AN SOA USING NONLINEAR POLARIZATION ROTATION 18

2.1 Introduction 19

2.2 Birefringence and nonlinear polarization rotation 20

2.3 Differential-phase-shift keying (DPSK) modulation format 22

2.4 Experimental setup 23

2.5 Experimental results 25

2.6 Conclusion 29

References 30

WIDEBAND SLOW LIGHT VIA STIMULATED BRILLOUIN SCATTERING IN AN OPTICAL FIBER USING A PHASE-MODULATED PUMP 32

3.1 Introduction 33

3.2 Stimulated Brillouin scattering (SBS) 34

3.3 Slow light via SBS 35

3.4 Experimental setup 37

3.5 Experimental result 39

Conclusion 42

References 43

SIGNAL WAVELENGTH TRANSPARENT SBS SLOW LIGHT USING XGM BASED WAVELENGTH CONVERTER AND BRILLOUIN FIBER LASER 45

4.1 Introduction 46

4.2 Brillouin fiber laser and XGM wavelength converter 47

4.3 Operating principle 50

4.4 Experimental setup and results 51

Conclusion 56

References 57

ALL-OPTICAL TUNABLE DELAY LINE FOR CHANNEL SELECTION IN A 40-GB/S OPTICAL TIME DIVISION MULTIPLEXING SYSTEM 59

5.1 Introduction 60

5.2 Principle of four-wave mixing 61

5.3 Channel selection in an OTDM system 63

5.4 Experimental setup 64

5.5 Experimental results 67

Conclusion 70

References 71

TUNABLE OPTICAL DELAY WITH CSRZ-OOK TO RZ-OOK OPTICAL DATA FORMAT CONVERSION USING FOUR-WAVE MIXING WAVELENGTH CONVERSION AND GROUP VELOCITY DISPERSION 73

6.1 Introduction 74

6.2 Carrier-Suppressed Return-to-Zero 76

6.3 Operating Principle 77

6.4 Experimental setup 79

6.5 Experimental result 81

Conclusion 86

References 87

CONCLUSION 90

7.1 Summary of work 90

7.2 Prospects of future work 92

APPENDIX: LIST OF PUBLICATIONS A

CHAPTER 1

Introduction

In a communication system, information is transferred between different locations. The transmission can vary from a few meters to hundreds of kilometers. Over the last 150 year, the transmission medium for long haul communications has changed from a single wire for telegraphy to a twisted wire for telephone, coaxial cable for TV-broadcasting and now optical fiber for broadband internet [1]. Light is used as the carriers of information in an optical communication system. The carrier is in the invisible or near-infrared region. The communication bandwidth has a frequency of ~ 100 THz.

The main application of optical fiber was limited to image transmission during the late 1960s. However, the situation changed dramatically in 1970 with the loss of silica fiber reduced to below 20 dB/km [2]. A further improvement in fabrication technology [3] resulted in a loss of 0.2 dB/km in the 1.55 μm wavelength region [4]. The loss was mainly limited by the fundamental process of Rayleigh scattering. Because of the high frequency of light, the bandwidth of optical communication is virtually unlimited (many tens of terahertz). Lucent's Allwave fiber opens a new window in optical communication at 1400 nm (see figure 1-1) [5]. The development in erbium-fiber-doped amplifier [6] enable optical transmission distance over a thousand kilometers. The main challenge in future optical network is to create ways of accessing the bandwidth of optical fiber. A transmission system with 640 Gb/s

has been investigated [7]. The bandwidth of optical fiber is well beyond the capacity of an electrical wire, therefore electronics create a limit to the speed of an optical communication network. Electrical signal processing is limited to a speed of 50 GHz and creates a bottleneck on operation. All-optical signal processing provides a solution to overcome the electronic limits. All-optical signal processing provides a potentially high speed and relatively inexpensive method for future communication networks.

Recently, all-optical tunable delay has attracted much research interest. All-optical tunable delay line is a fundamental building block in a modern communication network. A delay line is required for optical buffering or delaying signal in their processing at the bottleneck of an optical communication network. The traditional optical buffer requires optical-to-electrical and electrical-to-optical conversions that limit the bit-rate of the network. However, with the use of all-optical tunable delay line, the speed limit of electronics can be overcome. The delay line also enables other optical signal processing functions such as bit-level synchronization in an optical communication system.

In the following section, we will review different schemes to construct an all-optical tunable delay line. The schemes exhibit characteristics in terms of the maximum delay, the delay continuity, the pulse shape degradation, and the compactness.

1.1 Different ways to achieve all-optical tunable delay

1.1.1 Optical buffer realized with optical switching

A basic building block of an all-optical packet switched network is the optical buffer or memory. Optical fiber offers a trivial solution to optical buffering (propagation delay in optical fiber). A basic schematic illustration of an all-optical buffer is shown in figure 1-1 (a). The optical buffer is realized by using a combination of fiber delay lines and an all-optical switch. By controlling the routing of signal, the data packet can be switched to either pass- or buffer-port. The switch is usually realized by a wavelength converter and a WDM demultiplexer [8]. The buffer can be further extended to support different delays by using a 1 x N switch.

As the data length in the packet is of fixed length, the required storage time will be an integer multiple of the packet length. This allows the optical fiber loop to serve as an optical buffer. The schematic illustration of a fiber loop buffer is shown in figure 1-1 (b) [9]. To decide whether the data are being buffered or not, an optical switch is required. By controlling the number of circulations inside the fiber loop, the optical data can be buffered. A long buffer time can be achieved by increasing the number of circulations. The loss inside the fiber loop must be compensated in order to increase the buffering time. It can be done by placing an EDFA inside the fiber loop. However, the amplified spontaneous emission noise limits the performance of the optical buffer. Regeneration in the optical fiber loop buffer has been demonstrated to compensate the noise introduced by the amplification inside the fiber loop [10].

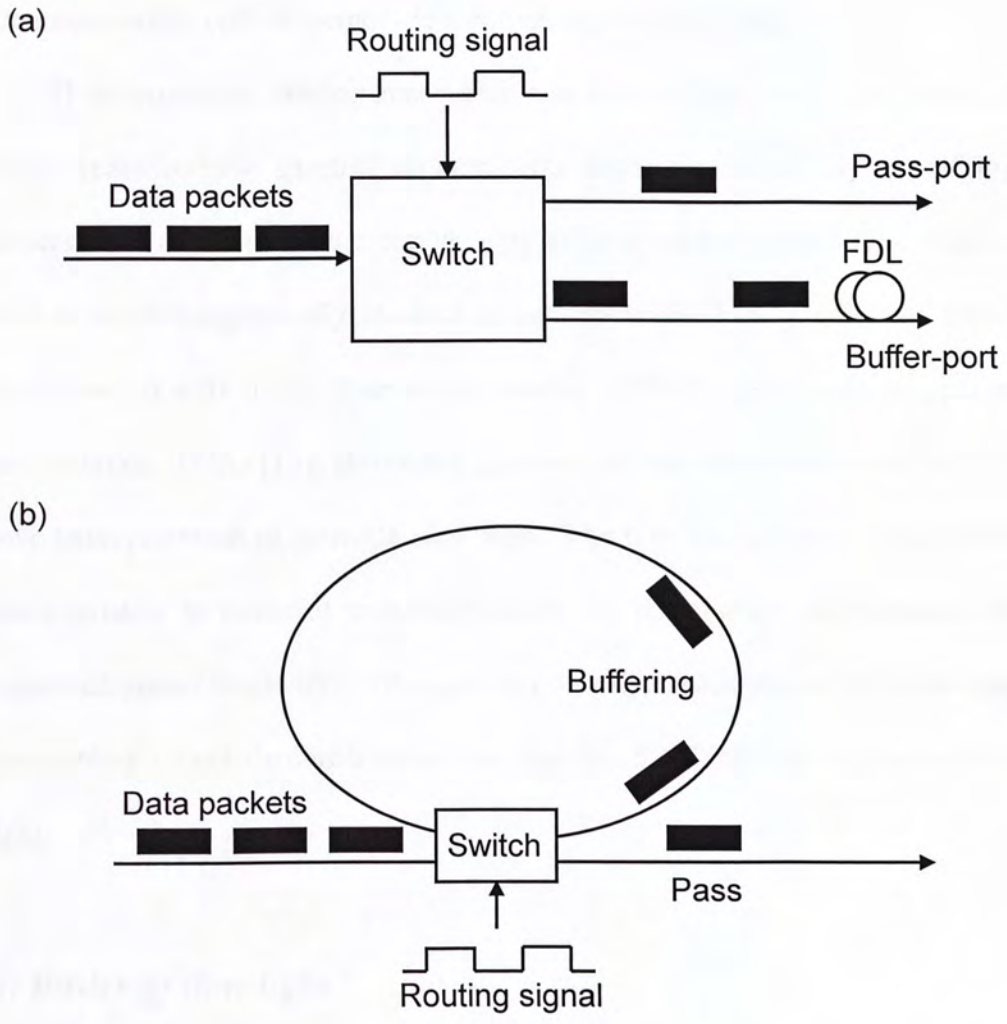

Figure 1-1: (a) Schematic illustration of optical buffer using switch and FDL; FDL: fiber delay line; (b) Schematic illustration of optical fiber loop buffer.

1.1.2 Slow light technique

Slow light is the literal slowing of the speed of light. It is the propagation of an optical pulse or other optical signal at a reduced group velocity. Recently, research at the nonlinear optics has demonstrated control over the speed of a light pulse as it propagates in a medium. It is possible to control the speed from its vacuum speed down to several meters per second [11]. Slow light techniques can be used to realize

optically controllable pulse delays for application such as optical buffering, data synchronization, optical memory and optical signal processing.

There are many mechanisms which can generate the slow light effect. All of them create narrow spectral regions with high dispersion. By modifying the dispersion of a medium, the group velocity of light can be reduced. The mechanisms such as electromagnetically induced transparency (EIT) [12], coherent population oscillation (CPO) [13], four-wave mixing (FWM) [14], optical parametric amplification (OPA) [15], stimulated Raman [16] and Brillouin scattering [17][18] have been proposed to generate slow light. The previous schemes exhibit different characteristics in terms of maximum delay, the pulse shape degradation, and the supported signal bandwidth. This sub-section offers background on slow light and summarizes recent demonstrations that employed different mechanisms for slow light.

(i) Basics of slow light

To understand the principle of slow light, it is crucial to realize that many different types of velocities characterize how an optical signal propagates through a medium. Considering a continuous-wave monochromatic (single frequency) beam of light with a frequency of ω_c, the phase velocity can be written as,

$$v_p = \frac{c}{n(\omega)} \tag{1.1}$$

where $n(\omega)$ is the frequency dependent index of refraction, c is speed of light in vacuum. The situation becomes complicated if an optical pulse rather than a CW light is propagating. From the basic Fourier theory, an optical pulse can be resolved into several frequency components. Therefore an optical pulse can be thought of as

resulting from constructive or destructive interference among different components. (see figure 1-2). In a material with frequency dependent refractive index, each of these components in the optical pulse propagates with different velocity. This results in a temporal shift of optical pulse with respect to the same pulse traveling in vacuum. The temporal shift of optical pulse implies that it is traveling at a different velocity. This is known as the group velocity (v_g) which is defined as

$$v_g = \frac{c}{n(\omega) + \omega \left.\frac{dn(\omega)}{d\omega}\right|_{\omega=\omega_c}} = \frac{c}{n_g} \tag{1.2}$$

where ω_c is the central frequency and n_g is the group index of the material. We can see that the group velocity depends on the dispersion of refractive index $dn/d\omega$.

Slow light effects make use of the rapid variation of refractive index associated with a material resonance. Slow light can be achieved when $v_g << c$. Vice versa, fast light can be achieved when $v_g >> c$. However, the pulse bandwidth has to be limited to the spectral region with the highly dispersive property.

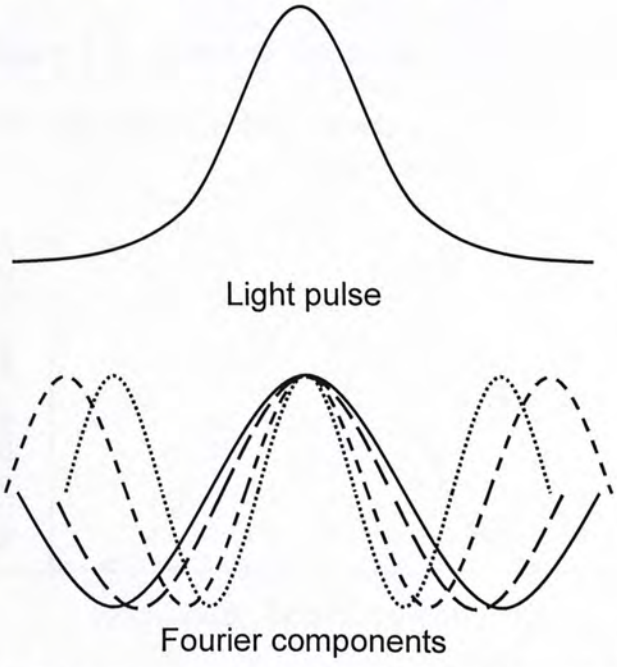

Figure 1-2: Fourier components wave interfere to create light pulse

(ii) Slow light via electromagnetically induced transparency (EIT)

Electromagnetically induced transparency (EIT) is coherent optical nonlinearity which can create a transparency (i.e. zero absorption) over a narrow spectral range with an absorption line. By Kramers-Kronig relations, an extreme dispersion is created simultaneously with this transparency. Therefore, slow light can be created in this spectral range. EIT is usually achieved in cold [19] or warm gases [20] of three level atoms. A group velocity down to 1 m/s is investigated with EIT [21]. Observation of EIT involves two optical waves (probe wave and pump wave) which are set to interact with the three level quantum states of a material. The probe wave is tuned near the resonance of two states and measures the absorption spectrum of the state transition. Another high intensity pump wave is tuned near the resonance at a different transition. If the state is coupled properly, the presence of pump wave will create a spectral region of transparency which can be seen by the probe wave. This results in an extremely low absorption (so-called transparency) at probe frequency. A rapid change of refractive index is associated with this reduced absorption. (see figure 1-3), therefore the group velocity of the probe wave is reduced dramatically. Thus, slow light is achieved.

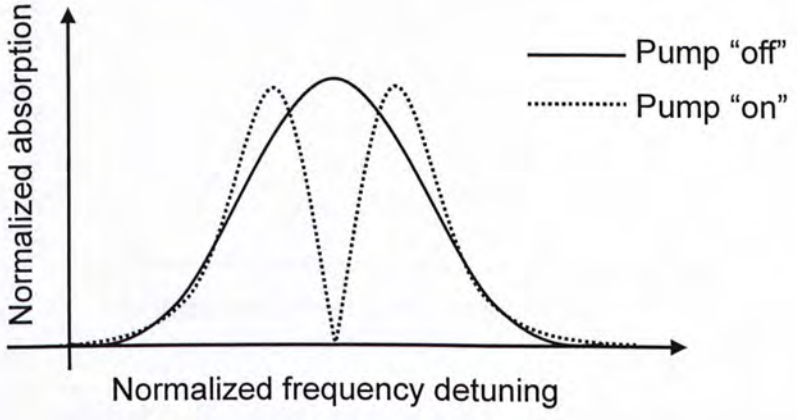

Figure 1-3: Change in absorption induced by EIT

(iii) Slow light via coherent population oscillation (CPO)

The EIT process involves two delicate quantum state transitions. These transitions can be destroyed with the presence of collisions or other phenomena. Thus the process cannot be observed at room-temperature which is desirable for practical applications in optical communication network. However, the process of coherent population oscillation (CPO) offers a solution.

When a strong pump wave (f_{pump}) and a probe wave (f_{probe}) of slightly different frequencies interact in a material that display saturable absorption. The population of ground state of the material will oscillate in time at the beat frequency of the two waves. This effect is known as CPO. The temporally modulated ground state scatters the pump wave. This contribution leads to decreased absorption in the probe frequency, this is, to a spectral hole in the probe absorption profile (see figure 1-4). A rapid change of refractive index is associated with the spectral hole. Thus, slow light is achieved at the probe frequency. The CPO has been demonstrated to slow down the speed of light in ruby crystal (display saturable absorption) [22].

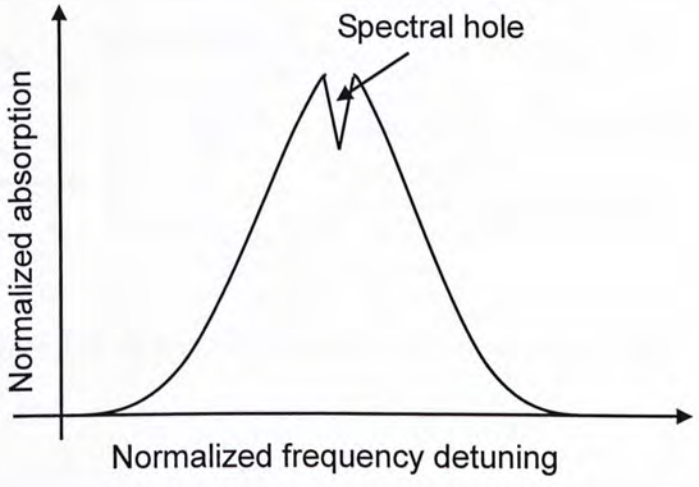

Figure 1-4: Spectral hole created by coherent population oscillation

(iv) Slow light via optical parametric amplification(OPA)

The previous slow light method has a fundamental limits related to the material, thus limiting the bandwidth and wavelength of operation [23]. Slow light can be achieved using fiber optics approach. Slow light have been demonstrated using optical parametric amplification (OPA). Using the narrow gain spectrum of OPA, slow light is achieved.

Near the zero-dispersion wavelength, amplification of light can be achieved by the energy transfer from a strong pump wave to the signal wave due to parametric process [24]. The schematic illustration of single pump OPA is shown in figure 1-5. An idler wave is generated simultaneously during the amplification. A gain over a narrow spectral range is created using a high gain and narrow band optical parametric amplifier [25]. A rapid change of refractive index is associated with the frequency dependent gain in the optical fiber generated by OPA. Thus, a reduction in group velocity (i.e. slow light) is resulted over the bandwidth of the amplifier. The group velocity can be controlled by adjust the parametric gain.

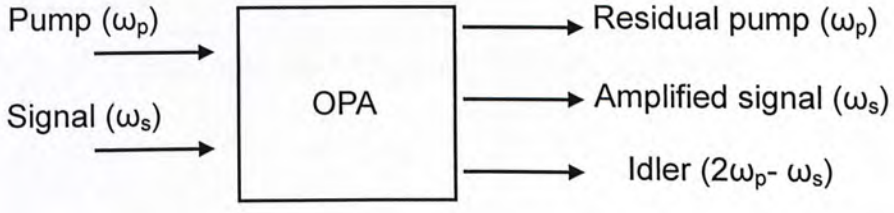

Figure 1-5: Schematic illustration of single pump OPA.

(v) Slow light via stimulated Raman and Brillouin scattering

The two most commonly observed forms of stimulated scattering are stimulated Brillouin scattering (SBS) and stimulated Raman scattering (SRS). SBS and SRS are

resulted from the high frequency acoustic wave and the vibration of optical phonons respectively. The schematic illustration of SBS and SRS slow light are shown in figure 1-6. These processes transfer light energy from the higher-frequency pump wave to the lower frequency one (Stokes wave), which results in exponential amplification of the signal wave when its frequency is detuned from the pump wave by the Stokes frequency. The amplification process is also accompanied by a rapid change of refractive index over a spectral range and gives rise to slow light. The slow light can be controlled by simply tuning the power of the pump wave. Controllable delays due to SBS and SRS offer an arbitrary wavelength of operation by simply changing the wavelength of the pump wave.

The intrinsic bandwidth of slow light via SBS is limited to several tens of MHz. However, the bandwidth can be pushed to 25 GHz [26] and supports the data rate in telecommunication network. Alternatively, the bandwidth of SRS is large enough to support very high data rate (~1 Tb/s). However, demonstration in optical C-band is not demonstrated due to lack of high power Raman pump.

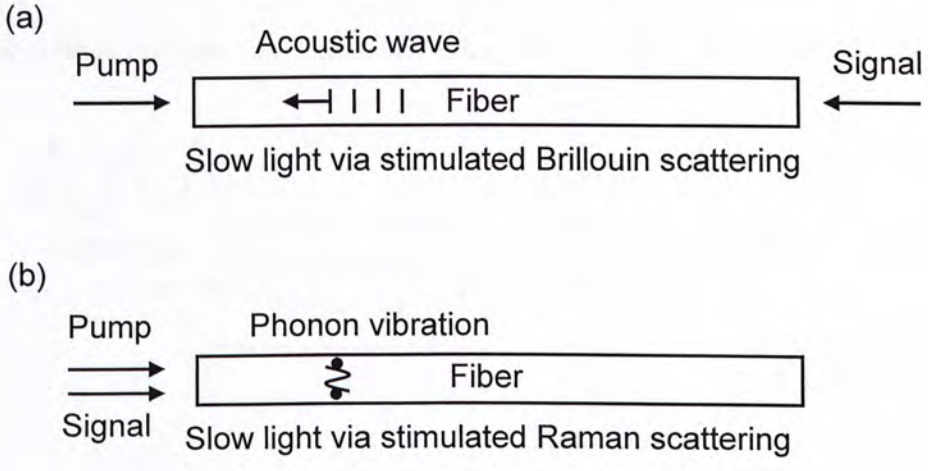

Figure 1-6: (a) Schematic illustration of slow light via SBS; (b) Schematic illustration of slow light via SRS.

1.1.3 Tunable delay using wavelength conversion together with chromatic dispersion

Apart from slow light techniques, all-optical wavelength conversion followed by signal propagation in a dispersive medium [27][28][29] presents as an alternative approach for tunable delay. The schematic illustration of the tunable delay is shown in figure 1-7. Unlike slow light which creates dispersion in a spectral region, the alternative approach creates a change in signal wavelength such that the signal propagates with a reduced group velocity caused by chromatic dispersion. The dispersive medium can be an optical fiber [30] or a chirped fiber Bragg grating (CFBG) [31]. Optical fiber provides a scalable dispersion according to its length and the dispersion can be compensated using dispersion compensating fiber which can minimize the effect on pulse distortion. However, the latency will increase dramatically using a long length of optical fiber as a dispersion medium. The latency can be reduced by using a chirped fiber Bragg grating which has a short length and large dispersion. Nevertheless, the transmission bandwidth of the CFBG limits the bandwidth of conversion, hence limits the maximum amount of delay.

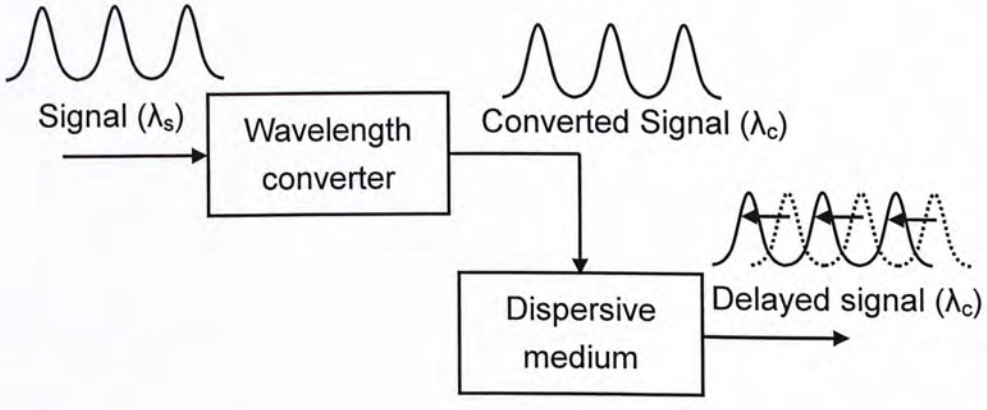

Figure 1-7: Schematic illustration of tunable delay using wavelength conversion together with chromatic dispersion.

1.1.4 Comparison of different schemes for constructing all-optical delay line

Different schemes for constructing all-optical delay line were reviewed in the previous session. Different characteristics of the schemes are summarized in the following table.

	Delay using all-optical switching	Slow light techniques	Wavelength conversion and dispersion
Mechanism	Switching between different propagation paths	Group velocity reduction generated by laser induced resonance	Group velocity change by different carrier wavelengths
Delay	Limited by signal attenuation	Limited by delay bandwidth product	Limited by the conversion bandwidth
Bandwidth	Switch speed	~1 THz (SRS)	Speed of wavelength converter
Delay continuity	Discrete	Continuous	Continuous
Setup	Complex	Relatively simple	Relatively simple

1.2 Overview of the thesis

The thesis mainly describes the different ways to achieve all-optical tunable delay for all-optical buffering or signal processing in future optical communication systems. The methods include switching of data signal to different optical propagation paths, slow light via SBS, tunable delay using wavelength conversion and chromatic dispersion as mentioned in Section 1.1.

In Chapter 2, we introduce the use of nonlinear polarization rotation (NPR) in a semiconductor optical amplifier (SOA) to perform switching of optical differential phase-shifted keying (DPSK) signal. A wavelength retaining 1 x 2 all-optical switch for DPSK signal built by commercial available components is presented here. The switch can be used for implementing optical delay by switching the DPSK signal to different optical propagation paths. The performances of the switch are discussed in Section 2.5.

Wideband continuously tunable delay via SBS slow light using a phase modulated pump is discussed in Chapter 3. SBS slow light is limited by a bandwidth of 30 MHz in an optical fiber. A phase modulated pump is used to broaden the gain bandwidth of the SBS to support telecommunication data rate (several Gb/s). The correlation between the required amount of phase modulation and the bandwidth of input signal pulses will be investigated.

In Chapter 4, we demonstrate an input signal wavelength transparent SBS slow light approach. A XGM wavelength converter and a Brillouin fiber laser are used in the demonstration. No alignment is needed between thepump wavelength and the signal wavelength. The working principle of the approach will be discussed in Section 4.3. A 40-nm wavelength transmission window with a maximum delay of 26 ns has been demonstrated and will be described in Section 4.4.

A tunable delay line constructed by FWM wavelength conversion and chromatic dispersion in a CFBG for fast channel selection in a 40-Gb/s OTDM system is discussed in Chapter 5. The OTDM signal is demultiplexed to 10-Gb/s in an electro-absorption modulator. With the use of the tunable delay line, synchronization and fast channel selection in an OTDM system is achieved. The performances of the setup are discussed in Section 5.5.

In Chapter 6, we presented an all-optical tunable delay with CSRZ-OOK to RZ-OOK conversion using pump modulated FWM wavelength conversion and group velocity dispersion. By exploiting the phase doubling characteristics of pump modulated FWM, CSRZ-OOK to RZ-OOK format and wavelength conversion is achieved. The details will be discussed in Section 6.2.

Finally, Chapter 7 summarizes my contribution during the master of Philosophy study. Prospects of future work will be discussed in this chapter.

References

[1] P. Cochrane, R. Heckingbottom, and D. Heatley, "The hidden benefits of optical transparency," IEEE Comms Mag., vol. 32, pp. 90-97 (1994).

[2] F. P. Kapron, D. B. Keck, and R. D. Maurer, "Radiation losses in glass optical waveguides," Appl. Phys. Lett., vol. 17, pp. 423-425 (1970).

[3] W. G. French, J. B. MacChesney, P. B. O'Connor, and G. W. Tasker, "Shuttle pulse measurements of pulse spreading in a low loss graded-index fiber," Bell Syst. Tech. J., vol. 53, pp. 951-953 (1974).

[4] T. Miya, Y. Terunuma, T. Hosaka, and T. Miyashita, "Ultimate low-loss single-mode fiber at 1.55 μm," Electron. Lett., vol. 15, pp. 106-107 (1979).

[5] G. Keiser, "Signal degradation in optical fibers," Ch. 3 in Optical Fiber Communications, (McGraw-Hill, 2000), pp. 91-140.

[6] E. Desurvire, J. Simpson, and P. C. Becker, "High-gain erbium-doped traveling-wave fiber amplifier," Opt. Lett., vol. 12, no. 11, pp. 888-890 (1987).

[7] F. Buchali, W. Baumert, M. Schmidt, and H. Bülow, "Dynamic distortion compensation in a 160 Gb/s RZ OTDM system: Adaptive 2 stage PMD compensation," in Proc. of OFC 2003, ThY1.

[8] C. Guillemot, M. Renaud, P. Gambini, C. Janz, I. Andonovic, R. Bauknecht, B. Bostica, M. Burzio, F. Callegati, and M. Casoni et al., "Transparent optical packet switching: The European ACTS KEOPS project approach," J. Lightw. Technol., vol. 16, pp. 2117-2134 (1998).

[9] R. Langenhorst, M. Eiselt, W. Pieper, G. Großkopf, R. Ludwig, L. Küller, E. Dietrich, and H. G. Weber, "Fiber loop optical buffer," J. Lightw. Technol., vol. 14, pp. 324-335 (1996).

[10] Srivastava, R.; Singh, R.K.; Singh, Y.N., "Regenerator based fiber optic loop memory," TENCON 2007 - 2007 IEEE Region 10 Conference , pp.1-4.

[11] D. Budker, D. F. Kimball, S. M. Rochester, and V. V. Yashchuk, "Nonlinear magneto-optics and reduced group velocity of light in atomic vapor with slow ground state relaxatoin," Phys. Rev. Lett. vol. 83, 1767-1769 (1999).

[12] S. E. Harris, J. E. Field, and A. Kasapi, "Dispersive properties of electromagnetically induced transparency," Phys. Rev. A, vol. 46, R29-R32 (1992).

[13] M. S. Bigelow, N. N. Lepeshkin, and R. W. Boyd, "Observation of ultraslow light propagation in a ruby crystal at room temperature," Phys. Rev. Lett., vol. 90, no. 11, p. 113 903 (2003).

[14] Zhangyuan Chen; Pesala, B.; Chang-Hasnain, C., "Experimental demonstration of slow light via four-wave mixing in semiconductor optical amplifiers," in Proc. of OFC/NFOEC 2006, OWS1.

[15] D. Dahan and G. Eisenstein, "Tunable all optical delay via slow and fast light propagation in a Raman assisted fiber optical parametric amplifier: a route to all optical buffering," Opt. Express, vol. 13, pp. 6234-6249 (2005).

[16] J. E. Sharping, Y. Okawachi, and A. L. Gaeta, "Wide bandwidth slow light using a Raman fiber amplifier," *Opt. Express*, vol. 13, pp. 6092–6098 (2005).

[17] K. Y. Song, M. G. Herraez, and L. Thevenaz, "Observation of pulse delaying and advancement in optical fibers using stimulated Brillouin scattering," Opt. Express vol. 13, pp. 82 - 88 (2005).

[18] Y. Okawachi, M. S. Bigelow, J. E. Sharping, Z. Zhu, A. Schweinsberg, D. J. Gauthier, R. W. Boyd, and A. L. Gaeta, "Tunable all-optical delays via Brillouin slow light in an optical fiber," Phys. Rev. Lett. vol. 94, no. 15, 153902 (2005).

[19] L. V. Hau, S. E. Harris, Zachary Dutton, and Cyrus H. Behroozi, "Light speed reduction to 17 metres per second in an ultracold atomic gas," Nature, vol. 397, pp. 594-598 (1998).

[20] M. M. Kash, V. A. Sautenkov, A. S. Zibrov, L. Hollberg, G. R.Welch, M. D. Lukin, Y. Rostovtsev, E. S. Fry, and M. O. Scully, "Ultraslow group velocity and enhanced nonlinear optical effects in a coherently driven hot atomic gas," Phys. Rev. Lett., vol. 82, pp. 5229–5232 (1999).

[21] C. Liu, Z. Dutton, C. H. Behroozi, and L. V. Hau, "Observation of coherent optical information storage in an atomic medium using halted light pulses," Nature 409, 490 (2001).

[22] M. S. Bigelow, N. N. Lepeshkin, and R. W. Boyd, "Observation of ultraslow light propagation in a ruby crystal at room temperature," Phys. Rev. Lett., vol. 90, pp. 113903 (2003).

[23] J. Mork, R. Kjaer, M. van der Poerl,L. Oxwenloewe and K. Yvind, "Experimental demonstration and theoretical analysis of slow light in a semiconductor waveguide at GHz frequencies," in Proc. of CLEO 2005, CMCC5.

[24] M. E. Marhic, N. Kagi, T.-K. Chiang, and L. G. Kazovsky, "Broadband fiber optical parametric amplifiers," Opt. Lett., vol. 21, pp. 573–575 (1996).

[25] E. Shumakher, A. Willinger, R. Blit, D. Dahan, and G. Eisenstein, "Large tunable delay with low distortion of 10 Gbit/s data in a slow light system based on narrow band fiber parametric amplification," Opt. Express, vol. 14, pp. 8540-8545 (2006).

[26] K. Y. Song and K. Hotate, "25 GHz bandwidth Brillouin slow light in optical fibers," Opt. Lett., vol. 32, pp. 217-219 (2007).

[27] J. E. Sharping, Y. Okawachi, J. van Howe, C. Xu, Y. Wang, A. E. Willner, and A. L. Gaeta, "All-optical, wavelength and bandwidth preserving, pulse delay based on parametric wavelength conversion and dispersion," Opt. Express, vol. 13, pp. 7872–7877 (2005).

[28] S. Oda and A. Maruta, "All-optical tunable delay line based on soliton self-frequency shift and filtering broadened spectrum due to self-phase modulation," Opt. Express, vol. 14, pp. 7895–7902 (2006).

[29] Mable P. fok and Chester Shu, "Tunable optical delay using four-wave mixing in a 35-cm highly nonlinear bismuth-oxide fiber and group velocity dispersion," J. Lightw. Technol., vol. 26, pp. 499-504 (2008).

[30] L. Christen, I. Fazal, O. F. Yilmaz, X. Wu, S. Nuccio, A. E. Willner, C. Langrock, and M. M. Fejer, "Tunable 105-ns optical delay for 80-Gbit/s RZ-DPSK, 40-Gbit/s RZ-DPSK, and 40-Gbit/s RZ-OOK signals using wavelength conversion and chromatic dispersion," in Pro.of OFC/NFOEC 2008, OTuD1.

[31] M. P. Fok and C. Shu, "Tunable pulse delay using four-wave mixing in a 35-cm bismuth oxide highly nonlinear fiber and dispersion in a chirped fiber Bragg grating," in Proc. of ECOC 2006, We1.3.3.

CHAPTER 2

All-optical switching of DPSK signal in an SOA using nonlinear polarization rotation

In this chapter, we introduce the use of nonlinear polarization rotation (NPR) in an semiconductor optical amplifier (SOA) to perform switching of optical differential phase-shifted keying (DPSK) signal. A wavelength retaining 1 x 2 all-optical switch for DPSK signal built by commercial available components is presented here. The switch can be used for implementing optical delay by switching the DPSK signal to different optical propagation paths. A 10-Gb/s NRZ-DPSK signal generated with 2^{31}-1 pseudorandom binary sequence (PRBS) is switched without changing its carrier wavelength. The switching utilizes NPR in an SOA. Using a polarization beam splitter (PBS), switching of DPSK signal can be achieved. The phase information of the DPSK signal is preserved throughout the switching process. The performance of the switch is characterized using a 10-Gb/s bit-error-rate (BER) tester. The measured power penalty is below 3 dB over a 12-nm operating wavelength.

2.1 Introduction

All-optical packet switched network [1] is a promising candidate for next generation optical communication network. Packet switching is a communication paradigm that information is split into discrete blocks of data packets. Packets are routed between nodes over data links shared with other traffic. By dividing the information into packets, the transmission bandwidth can be fully utilized by statistically sharing the data links, giving rise to high capacity communication with improved efficiency and flexibility. Optical header processing [2][3], optical packet switching [4], and optical buffering [5][6] are involved in an all-optical packet switched network The crucial component for the network is an all-optical switch or router. Optical buffering and packet switching require an ultra-fast all-optical switch. Optical buffering or delay can be constructed by switching the data packet to different optical propagation paths or to a fiber loop for achieving different delay. A common approach to perform switching is to use all-optical wavelength conversion together with an array waveguide grating (AWG). The approach is able to perform N x N switching, however, an unavoidable change in carrier wavelength is associated. Recently, the differential phase-shift keying (DPSK) [7] optical data format has received much attention compared to the conventional on-off-keying (OOK) or amplitude-shift keying (ASK) data format. With the use of balance detection, DPSK signal offers a 3-dB improvement in receiver sensitivity compared to ASK signal. The gain saturation effect in amplifier that may degrade the ASK signal is less detrimental to DPSK signal. In addition, the low peak power and the uniform distribution of power in every bit of NRZ-DPSK signal imply that it is more resilient to fiber nonlinearity. Channels cross talk and signal degradation from four-wave mixing and nonlinear phase modulation can be minimized. However, phase

information is not preserved in most of the common wavelength conversion techniques, such as cross-gain modulation and cross-phase modulation. Hence, the techniques are not compatible for switching and buffering of DPSK signal.

To demonstrate switching of DPSK signal without changing the signal carrier wavelength, we propose to use nonlinear polarization rotation (NPR) induced by cross-phase modulation (XPM) in a semiconductor optical amplifier (SOA). NPR can be applied for wavelength conversion [8][9] but is also capable for switching when used with a polarization selective element such as a polarizer or a polarization beam splitter. In this chapter, we demonstrate a 1 x 2 optical switch for 10-Gb/s NRZ-DPSK signal using commercially available components. The optical switch rotates the polarization of the incoming signal through NPR at the SOA without converting the signal wavelength. Phase information of the DPSK signal is preserved throughout the process. The switch can be used to implement tunable delay line by switching the signal to different optical propagation paths. The switched signal is characterized by bit-error-rate (BER) measurement. A power penalty of less than 3 dB is obtained across a 12-nm operating range.

2.2 Birefringence and nonlinear polarization rotation

Birefringence or double refraction is the decomposition of light into two rays (the ordinary ray and extraordinary ray) when it passes through certain materials. The two light rays have different polarizations. In an optical fiber, the two different indices of refraction in different polarization directions result in different propagation

speed of light for different directions. The birefringence [10][11][12] is defined by

$$\Delta n = n_e - n_o \tag{2.1}$$

where n_e is the extraordinary refractive index for light electric field parallel to the optic axis and n_o is the ordinary refractive index for light with electric filed perpendicular to the optic axis.

Figure 2-1 shows the schematic illustration of an optical kerr shutter [13]. The pump and probe beams are linearly polarized at the nonlinear medium input with a 45° angle between their polarization directions. A crossed polarizer blocks probe transmission in the absence of the pump beam at the output of the nonlinear medium. When the pump is turned on, the refractive indices for the parallel and perpendicular components of the probe (with respect to the direction of pump polarization) become slightly different because of pump-induced birefringence. The phase difference between the two components at the nonlinear medium output manifests as a change in the probe polarization, and a portion of the probe intensity is transmitted through the polarizer. The probe transmittivity depends on the pump intensity and can be controlled simply by changing the intensity. As the probe output at one wavelength can be modulated through a pump at a different wavelength, this device is also referred to as the Kerr modulator and has attracted considerable attention [14][15][16][17]. It is found useful in fiber-optical networks requiring all-optical switching.

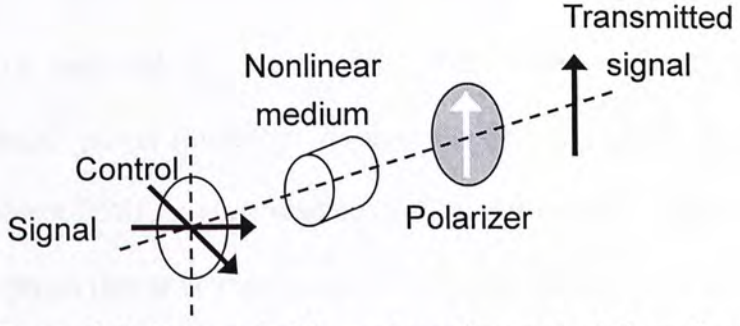

Figure 2-1: Schematic illustration of an optical Kerr shutter

2.3 Differential-phase-shift keying (DPSK) modulation format

A number of advanced optical modulation formats have been proposed to enhance the robustness of signal to chromatic dispersion, optical filtering, and fiber-nonlinearities as described in [7]. In particular, phase-shift-keyed formats have attracted much research attention. Binary-phase-shift-keyed (BPSK) formats carry the information in the phase itself. Because of the lack of an absolute phase reference in receivers, the phase of the preceding bit is used as a relative phase reference for demodulation. This gives rise to differential-phase-shift-keyed (DPSK) formats, which carry the information in optical phase changes between bits.

In the DPSK format, optical power appears in every bit slot, with the binary data encoded as either a 0 or π optical phase shift between adjacent bits. The optical power in each bit can occupy the entire bit slot (NRZ-DPSK) or appears as an optical pulse (RZ-DPSK). The most significant advantage of DPSK format compared to ASK format is the 3-dB reduction in the required signal to noise ratio to achieve the same bit-error-rate (BER). This can be understood by comparing the signal constellations for DPSK and ASK signal as shown in figure 3-2. For the same average power, the symbol distance in DPSK is increased by $\sqrt{2}$. Therefore, only half optical power is required to achieve the BER. The 3-dB benefit of DPSK can be extracted using balanced detection. DPSK with balanced detection offers large tolerance to signal power fluctuation because the decision threshold is independent of the input power DPSK is more resilient to fiber nonlinearity. This results from the fact that the optical power is more evenly distributed than in ASK (power is present in every bit slot for DPSK, which reduces bit-pattern-dependent nonlinear effects)

and the optical peak power is 3 dB lower for DPSK than for ASK for the same average power.

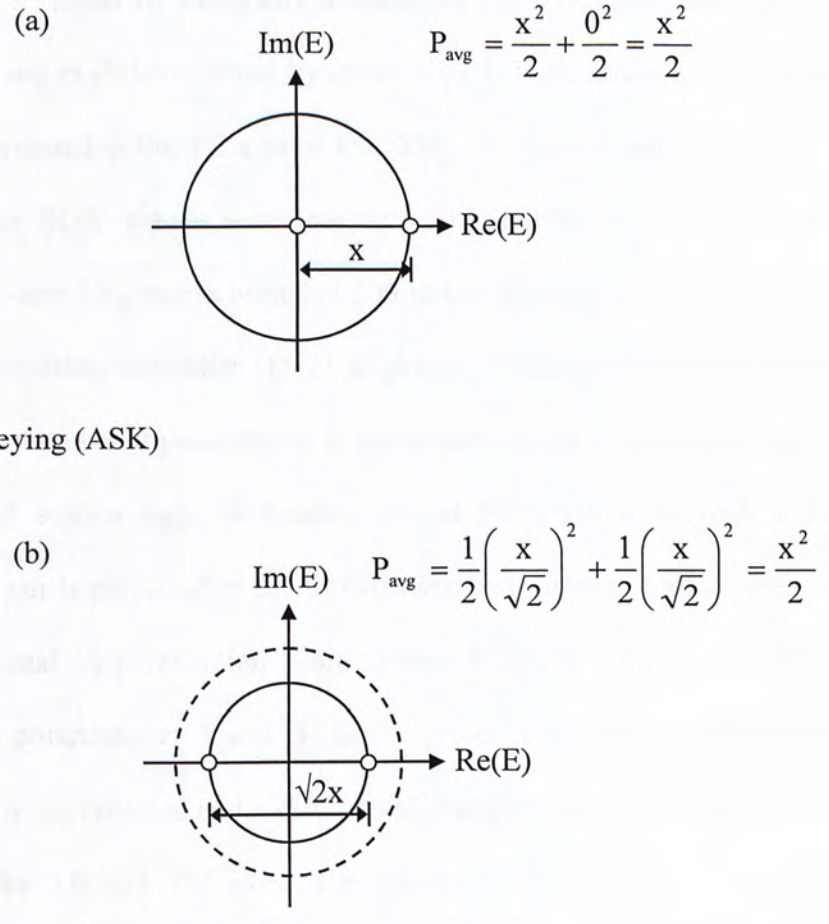

Figure 2-2: Signal constellation of (a) ASK format; (b) DPSK format.

2.4 Experimental setup

The experimental setup of the proposed 1 x 2 optical switch for DPSK signal is shown in figure 2-3. A 1555.4-nm laser diode is externally modulated by a phase modulator to generate a 10-Gb/s NRZ-DPSK signal. A polarization controller (PC1) is used to adjust the signal polarization. The signal is linearly polarized and is oriented at 45° with respect to the TE axis of the SOA. The polarization of the signal

being coupled is first adjusted by monitoring the polarization dependence of the gain characteristic of the SOA. Once the input signal polarization is set, it is kept unchanged throughout the experiment. The average power of the signal is -6.8 dBm. A control light is prepared by externally modulating a CW tunable laser using an electro-optic intensity modulator driven by an RF signal. The control light is linearly polarized and is oriented at the TE axis of the SOA. The signal and the control are launched into the SOA via a 3-dB coupler. The nonlinear SOA (Kamelian NL-H1-C-FA) is 1-mm long and is biased at 200 mA to produce a gain peak at 1563 nm. Another polarization controller (PC2) is placed at the output of the SOA to maximize the signal power at polarization A while minimizing that at polarization B in the absence of control light. A tunable optical bandpass filter with a 3-dB bandwidth of 0.4 nm is placed after the polarization controller to block the control beam from the signal. A polarization beam splitter (PBS) is used to provide two output ports with polarizations A and B. In the presence of the control light, the carriers in the SOA are depleted and a differential change in the refractive indices is produced along the TE and TM axes. The change in birefringence results in a polarization rotation of the signal. The signal beam is therefore switched to another port of the PBS with an output at polarization B. As the phase change induced on every bit of the DPSK signal is constant, the differential phase information of the DPSK is preserved. A 100-ps delay interferometer (DI) is used to demodulate the DPSK signal before the bit-error-rate (BER) measurement is performed.

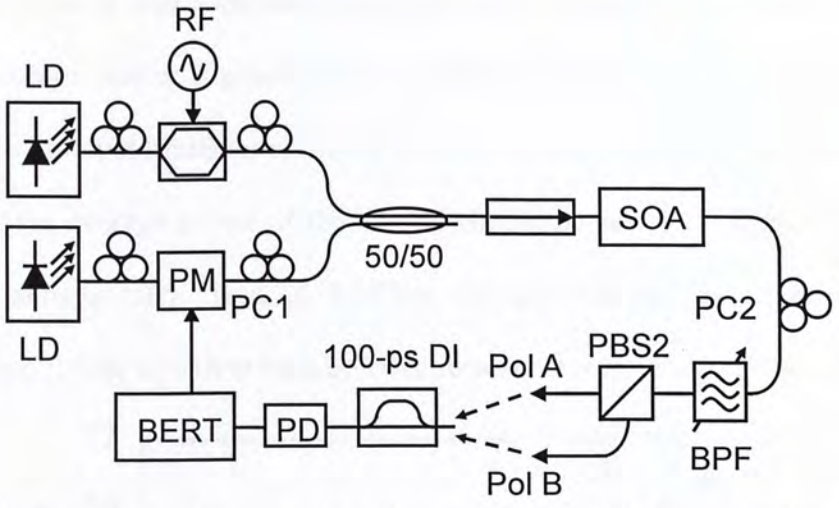

Figure 2-3: Experimental Setup of 1 x 2 optical switch. LD: laser diode; PM: phase modulator; 50/50: 3-dB coupler; PC1, PC2: polarization controller; SOA: semiconductor optical amplifier; BPF: optical bandpass filter; PBS: polarization beam splitter; Pol A: polarization A; Pol B: polarization B; DI: delay interferometer; PD: Photodiode; BERT: bit-error rate tester

2.5 Experimental results

To optimize the switching performance, a CW light is first used as the control beam. The extinction ratio is defined as the ratio of the signal powers at the output with and without the control beam. The dependence of the output signal extinction ratio on the control light power is shown in figure 2-4 (a). Both output ports of the PBS with signals at polarization A and polarization B are studied. Apart from nonlinear polarization rotation, the gain of the SOA is also depleted by the control light, resulting in different extinction ratios at the two polarizations. When the control power increases, the carrier depletion at the SOA is more pronounced. Thus, the signal power in its "off" state at polarization A is further suppressed and leads to an enhancement in the extinction ratio. However, the output signal at polarization B

in its "on" state is also suppressed and leads to a reduction in the extinction ratio when the control power is greater than 1.2 dBm. To obtain the same extinction ratio of 9.5 dB at both polarizations as shown in the intersection point of the two curves in Fig. 3 (a), the average power of the control should be set at 1.7 dBm. The control power is subsequently fixed at 1.7dBm for the rest of the experiment. The demodulated DPSK signals at both polarizations are shown in figure 2-4 (b).

(a)

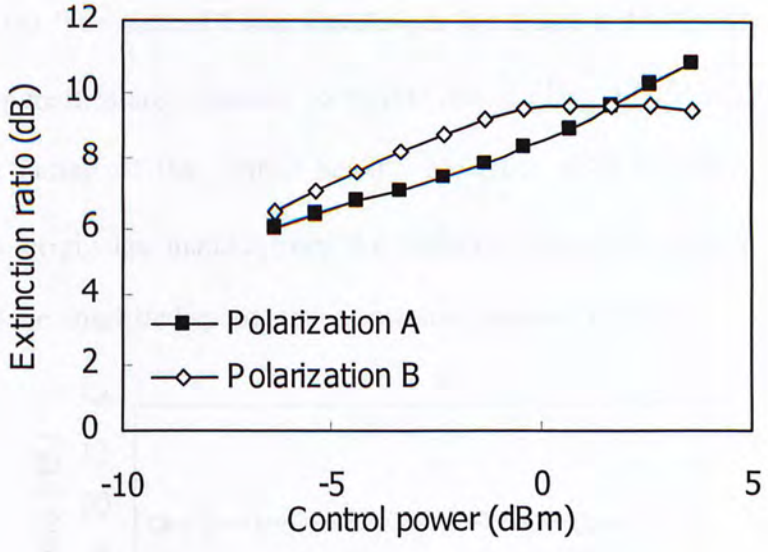

(b)

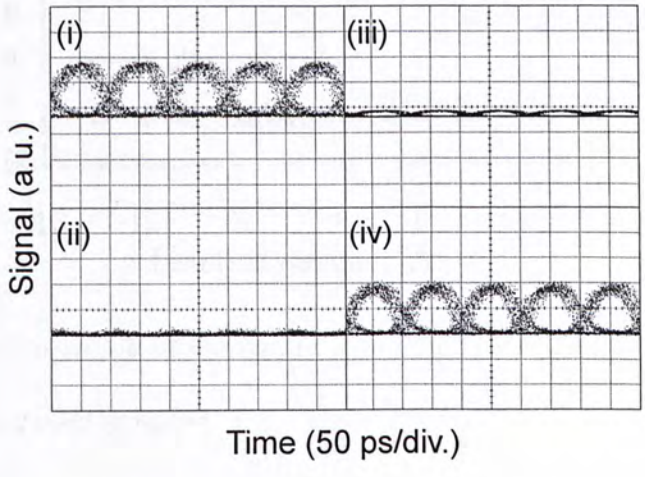

Fig. 2-4: (a) Signal extinction ratios against the control power at the output ports of the polarization beam splitter. (b): (i) Output of polarization A at "on" state. (ii) Output of polarization A at "off" state. (iii) Output of polarization B at "on" state. (iv) Output of polarization B at "off" state.

Fig. 2-5 shows the change of the extinction ratio by detuning the control over a range of 20 nm. The extinction ratio variation is less than 0.3 dB throughout the tuning range. The result indicates that the wavelength difference between the control and the signal can be widely tuned without affecting the performance of the switch. To investigate the performance of optical switching of DPSK signal, 10-Gb/s BER measurements are performed at both ports using 2^{31}-1 PRBS. The results are shown in Fig. 2-6 (a). The control beam wavelength is chosen at 1545, 1556, or 1560 nm. The power penalties are measured to be less than 3 dB at a BER of 10^{-9} over 12-nm wavelength tuning of the control beam. No BER floor is observed. The signal degradation originates mainly from the reduced extinction ratio of the switched outputs and the amplified spontaneous emission noise of the SOA.

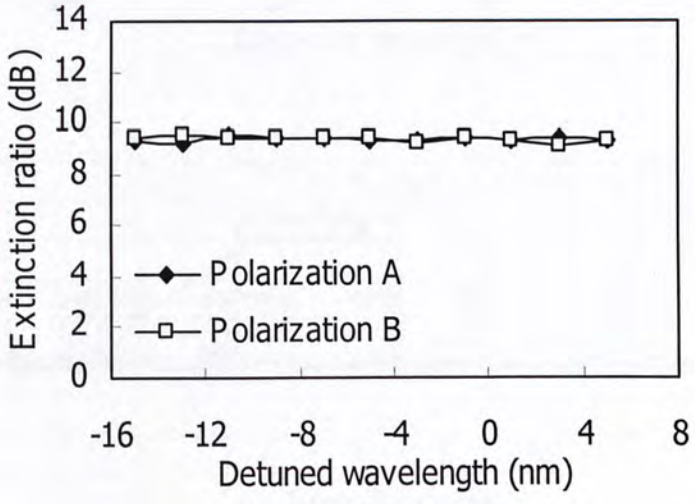

Fig. 2-5: Extinction ratios of the output signals at polarizations A and B over a 20-nm wavelength detuning range.

To study the switching behavior with a modulated control beam, we use a 6-MHz square wave producing 50-ns wide pulses with a duty cycle of 30%. The output switched waveforms at polarization A and polarization B are shown in figure 2-6 (b). The insets in figure 2-6 (b) correspond to demodulated DPSK signal eyes at

the output of the PBS. Clear and widely open eyes are observed after the switching, thus supporting use of the compact 1 x 2 switch for DPSK signal switching in a real network.

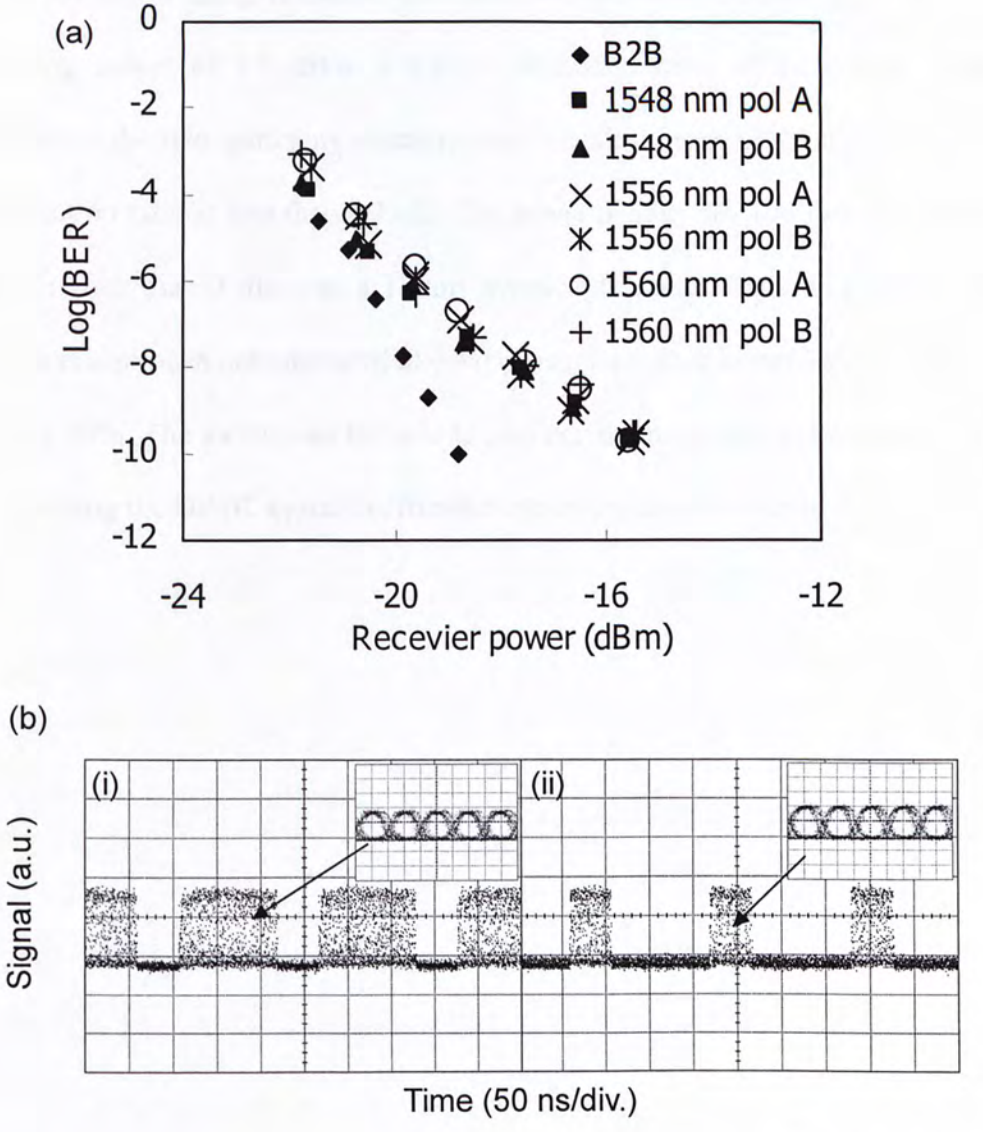

Figure 2-6: (a) BER measurement results for signals at polarization A and polarization B with 12-nm control wavelength detuning. (b): (i) Switched waveform at polarization A. (ii) Switched waveform at polarization B. Insets: Corresponding eye diagrams of the switched waveforms.

2.6 Conclusion

In this chapter, we demonstrate a wavelength-retaining, all-optical 1 x 2 switch for DPSK signal using nonlinear polarization rotation in a SOA. With an average switching power of 1.7 dBm, a 9.5-dB extinction ratio of the output signal is achieved at the two switching outputs. Over a tuning range of 20 nm, the variation of extinction ratio is less than 0.3 dB. The power penalty for 10-Gb/s data at a BER of 10^{-9} is less than 3 dB over a 12-nm wavelength range. Switching of the DPSK signal has also been demonstrated at 6 MHz using a square control pulse with a duty cycle of 30%. The switch can be used to implement an all-optical tunable delay line by switching the DPSK signal to different optical propagation paths.

References

[1] D. J. Blumenthal, P. R. Prucnal, and J. R. Sauer, "Photonic Packet Switches: Architectures and Experimental Implementations," Proc. IEEE., vol. 82, pp. 1650-1667 (1994).

[2] J. M. Martinez, Y. Liu, R. Clavero, A. M. J. Koonen, J. Herrera, F. Ramos, H. J. S. Dorren, and J. Marti, "All-Optical Processing Based on a Logic XOR Gate and a Flip-Flop Memory for Packet-Switched Network," IEEE Photon. Technol. Lett., vol. 19, pp. 1316-1318 (2007).

[3] M. T. Hill, A. Srivatsa, N. Calabretta, Y. Liu, H. D. Waardt, G. D. Khoe, and H. J. S. Dorren, "1x2 Optical Packet Switch Using All-Optical Header Processing," Electron. Lett., vol. 37, pp. 774-775 (2001).

[4] J. Herrera, E. Tangdiongga, Y. Liu, M. T. Hill, R. McDougall, A. Poustie, G. Maxwell, F. Ramos, J. Marti, H. de Warrdt, G. D. Khoe, A. M. J. Koonen, and H. J. S. Dorren, "160-Gb/s All-Optical Packet-Switching With In-Band Filter-Based Label Extraction and a Hybrid-Integrated Optical Flip-Flop," IEEE Photon. Technol. Lett., vol. 19, pp. 990-992 (2007).

[5] Haijun Yang and S. J. Ben Yoo, "All-Optical Variable Buffering Strategies and Switch Fabric Architectures for Future All-Optical Data Routers," IEEE J. Lightw. Technol., vol. 23, pp. 3321-3330 (2005).

[6] Yajie Li, Chongqing Wu, Songnian Fu, P. Shum, Yandong Gong, and Liren Zhang, "Power Equalization for SOA-Based Dual-Loop Optical Buffer by Optical Control Pulse Optimization," IEEE Quant. Electron., vol. 43, pp. 508-516 (2007).

[7] A. H. Gnauck and P. J. Winzer, "Optical Phase-Shift-Keyed Transmission," IEEE J. Lightw. Technol., vol. 23, pp. 115-130 (2005).

[8] Ju Han Lee and Kazuro Kikuchi, "All-Fiber 80-Gbit/s Wavelength Conversion Using 1-m-long Bismuth Oxide-Based Nonlinear Optical Fiber with a Nonlinearity γ of 1100 $W^{-1}km^{-1}$," Opt. Exp., vol. 13, pp. 3144-3149 (2005).

[9] C. S. Wong and H. K. Tsang, "High Extinction Ratio Wavelength Conversion at 10 Gbit/s using Birefringence Switching in Semiconductor Optical Amplifier," Electron. Lett., vol. 16, pp. 897-898 (2002).

[10] P. Yeh and C. Gu, "Jones matrix method," Ch. 1 in Optics of liquid crystal displays, (New York: Wiley, 1999), pp. 1-21.

[11] G. P. Agrawal, "Introduction," Ch. 1 in Nonlinear fiber optics, (Academic Press, 3 rd Ed., 2001), pp. 1-30.

[12] I. P. Kaminow, "Polarization in optical fiber," IEEE J. Quantum Electron. Vol. 17, pp. 15-22 (1981).

[13] M. A. Duguay and J. W. Hansen, "An ultrafast light gate," Appl. Phys. Lett., vol. 15, pp.192-194 (1969).

[14] R. H. Stolen and A. Ashkin, "Optical Kerr effect in glass waveguide," Appl. Phys. Lett., vol.22, pp. 294-296 (1973)

[15] K. Kitayama, Y. Kimura, K. Okamoto, and S. Seikai, "Optical sampling using an all-optical Kerr shutter," Appl. Phys. Lett., vol. 46, pp. 623-625 (1985)

[16] I. H. White, R. V. Penty, and R. E. Epworth, "Demonstration of the optical Kerr effect in an all-fiber Mach-Zehnder interferometer at laser diode powers," Electron. Lett., vol. 24, pp. 340-341 (1988)

[17] M. Asobe, T. Kanamori, and K. Kubodera, "Ultrafast all-optical switching using nonlinear chalcogenide glass fiber," IEEE Photon. Technol. Lett., vol. 4, pp. 362-365 (1992)

CHAPTER 3

Wideband slow light via stimulated Brillouin scattering in an optical fiber using a phase-modulated pump

In previous chapter, we demonstrate all-optical switching using nonlinear polarization rotation. The switch can be used to implement tunable delay line by switching the input signal to different optical propagation paths. However, the achieved delay is only discretely tunable. To achieve continuously tunable delay, slow light via stimulated Brillouin scattering (SBS) is proposed. However, SBS slow light technique has its limitation in bandwidth. The intrinsic Brillouin linewidth is restricted to approximately 30 MHz in conventional single mode fiber and therefore the useful data rate is limited to several tens of Mb/s. It is much lower than the data rate (in the orders of Gb/s) in optical communication. In this chapter, we investigate slow light via SBS in a room temperature optical fiber that is pumped by a phase-modulated pump. Broadening the spectrum of pump field increased the linewidth of the Stokes amplifying resonance, thereby increasing the slow light bandwidth to delay 26-ps pulses.

3.1 Introduction

There has been great interest in slowing the propagation speed of optical signal (so-called slow light) using different optical methods [1]. Slow light technique can be used to perform many functions for future optical communication networks, including optical buffering, data synchronization and signal processing [2][3][4]. Slow light is usually achieved with resonant effects that create a large normal dispersion in a narrow spectral region, which increases the group index and results in a reduction in group velocity of the optical signal. Optical resonance associated with stimulated Brillouin scattering (SBS) [5][6], stimulated Raman scattering (SRS) [7], and parametric amplification [8] in an optical fiber have been recently demonstrated to achieve slow light.

The spectral width of resonance limits the time duration of the optical pulse. For a narrow optical pulse, a larger width of resonance is required. In this regard, slow light in optical fiber via SBS is limited to data rate in the order of tens of Mb/s due to the narrow linewidth of SBS (~ 30 MHz for standard single mode fiber). Recently, SBS slow light bandwidth has been increased to about 12 GHz by broadening the spectrum of the SBS pump field using an intensity modulated pump [9]. In this chapter, optical pulses train at both 1 GHz and 10 GHz are delayed using SBS with a phase modulated pump. We also investigate the effect of the linewidth of pump on slow light. The phase modulated pump provides a constant pump power and thus no synchronization is needed between the pump and signal pulses. Hence, the approach offers a practical means in amplifying and delaying high-bit-rate pulses (up to 10 GHz) and true data in communication network.

3.2 Stimulated Brillouin scattering (SBS)

Stimulated Brillouin scattering (SBS) has been studied extensively in the past few decade. The SBS process generates a Stokes wave down-shifted from the frequency of the incident pump wave by an amount determined by the nonlinear medium. The Stokes wave propagates backward when SBS occurs in an optical fiber. The Stokes shift of SBS in an optical fiber is around 10 GHz and the threshold pump power for SBS depends on the spectral width associated with the pump wave. The process of SBS can be described classically as the interactions among the pump wave, the Stokes wave, and an acoustic wave. The pump wave generates acoustic waves through the process of electrostriction which in turn causes a periodic modulation of the refractive index. The pump-induced index grating scatters the pump light through Bragg diffraction and generates the backward propagating Stokes wave. The Stokes wave is down-shifted in frequency because of the Doppler shift associated with a grating moving at acoustic velocity. The Brillouin shift of the Stokes wave is given by,

$$\nu_B = \frac{\Omega_B}{2\pi} = \frac{2n\nu_A}{\lambda_p} \tag{3.1}$$

where n is the modal index at pump wavelength λ_p and ν_A is the acoustic velocity. The growth of the Stokes wave can be characterized by the Brillouin-gain coefficient of which the peak value occurs at ν_B. The Brillouin gain of an optical fiber can be used to amplify a weak signal with a frequency shifted from the pump frequency by an amount equal to the Brillouin shift. However, because of an extremely narrow Brillouin-gain profile (< 100 MHz), the bandwidth of such amplifiers is generally below 100 MHz. For this reason, fiber-Brillouin amplification does not attract much attention compared to Raman amplification even

though amplification can be achieved with only a few milliwatts pump power.

3.3 Slow light via SBS

SBS can be treated as a narrowband amplification process, in which a strong pump wave produces a narrowband gain region and another narrowband loss region. According to the Kramers-Kronig relation, a rapid change of refractive index is associated with the Brillouin gain/loss process and a substantial change of the group index $n_g = n + \omega dn/d\omega$ follows as a result of sharp index change. The plots in figure 3-1 shows the frequency dependence of the SBS gain, refractive index change, and group index change. From figure 3-1, positive group index change is observed near the peak of gain resonance, which indicates a reduction in group velocity. Vice versa, an increase in group velocity is observed at the region of negative group index change. Therefore an increase in group velocity is obtained (so-called fast light).

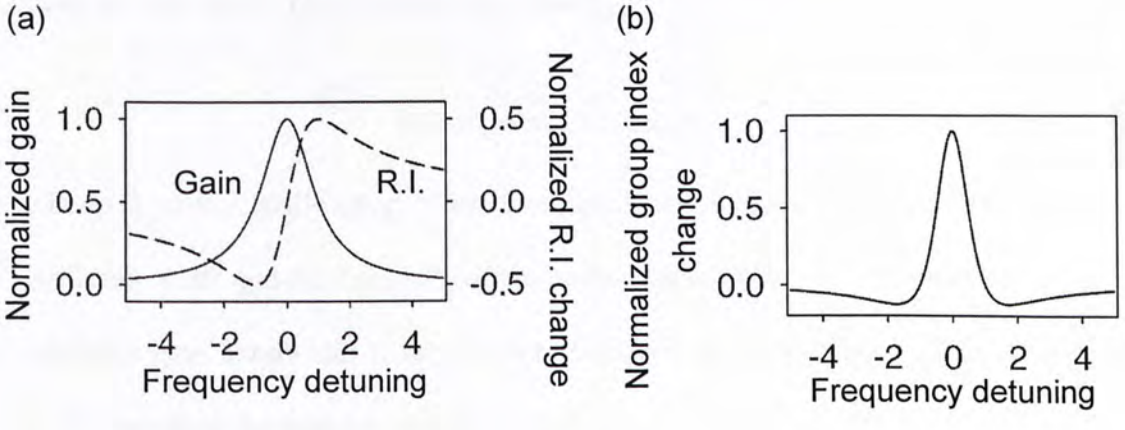

Figure 3-1: (a) Plot of normalized SBS gain and normalized refractive index change against frequency detuning; (b) Plot of normalized group index change against frequency detuning

When a laser pump with a single frequency is used in the generation of SBS,

the Brillouin gain window appearing in the optical fiber has a Lorentzian shaped spectral profile with a spectral width of 30 MHz in conventional single mode fiber. However, when the pump is modulated the Brillouin gain bandwidth is given by the convolution between the pump spectrum and the intrinsic Brillouin gain spectrum $g(\Delta\nu)$ and is given by [10],

$$g(\Delta\nu) = P(\Delta\nu) \otimes g_B(\Delta\nu) \tag{3.1}$$

where $\otimes$ donotes convolution, $P(\Delta\nu)$ is the normalized pump power spectral density and $g_B(\Delta\nu)$ is the characteristic Lorentzian gain of Brillouin amplification process. Hence the pump modulation can be used to broaden the gain bandwidth of SBS. The SBS gain spectrum can be controlled by changing the spectral shape of the pump. If the pump spectrum can be approximated by a Lorentzian, the effective Brillouin gain spectrum remains Lorentzian but shows a width equal to the sum of the intrinsic Brillouin gain bandwidth and the pump spectral width. In this particular case, the time delay (T_d) obtained is given by,

$$T_d = \frac{G}{2\pi(\Delta\nu_B + \Delta\nu_P)} \approx \frac{G}{2\pi\Delta\nu_P} \tag{3.2}$$

where G is the Brillouin gain on the signal and $\Delta\nu_B$ and $\Delta\nu_P$ are characteristic Brillouin width and the linewidth of the pump, respectively. For RZ-OOK signal, the optimize gain bandwidth without much distortion is around twice of the data rate [11]. Therefore the equation can be written as,

$$T_d \approx \frac{G}{2\pi(2B)} \tag{3.3}$$

where B is the bit rate of the RZ-OOK signal. For a fixed Brillouin gain, the delay is reduced as a double speed with increasing signal bit rate. Theoretically, the delay can be increased by enhancing the Brillouin gain. However, the dependence between the Brillouin gain and pump linewidth is not consider in this equation. In real case,

the Brillouin threshold increases with pump modulation rate. Therefore, the maximum delay is also limited by the maximum Brillouin gain achieved in the system.

3.4 Experimental setup

The setup of SBS slow light using a phase-modulated pump is shown in figure 3-2. A 1551.318-nm laser diode is modulated by an electro-optic intensity modulator (EOM) to produce the input signal pulses. The polarization controller (PC1) is used to optimize the intensity modulation. Modulation rates at both 1 GHz and 10 GHz are used to generate pulses with different time duration in the experiment. The signal pulses are amplified using an erbium-doped-fiber amplifier (EDGA) to give an average power of 0 dBm and is launched into an 8-km standard single mode fiber (SMF-33) through an optical isolator. The measured Brillouin shift of the SMF-33 single mode fiber is approximately 0.088 nm, as shown in figure 3-3.

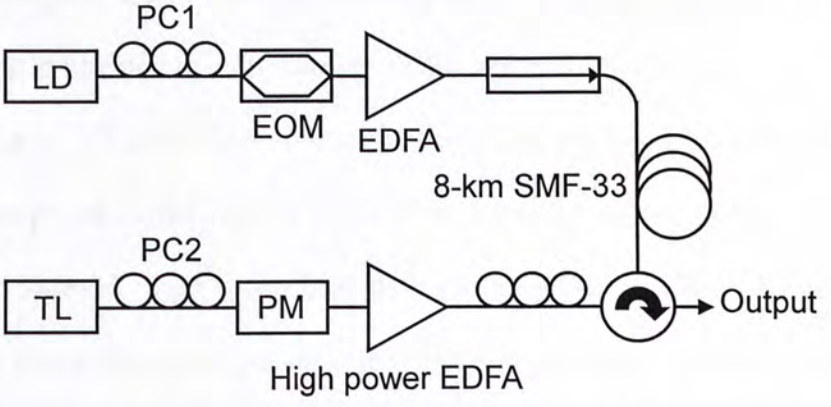

Figure 3-2: Experimental of SBS slow using a phase-modulated pump. LD: laser diode; PC1 and PC2: polarization controller; EOM: electro-optic intensity modulator; PM: phase modulator; EDFA: erbium-fiber-doped amplifier; SMF: standard single mode fiber.

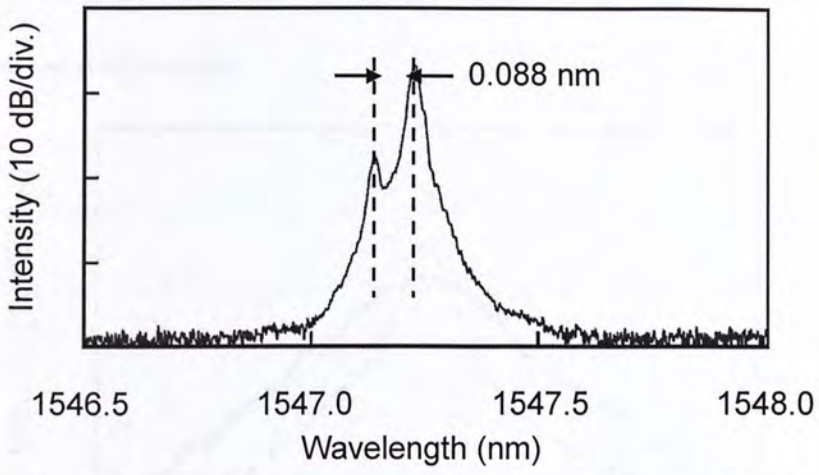

Figure 3-3: Measured Brillouin shift of SMF-33 standard single mode fiber

Another tunable CW laser is used as a pump light. The laser is set to operate at 1551.230 nm (1551.318 -0.088 nm) such that the generated Brillouin gain is exactly aligned with the wavelength of signal pulse. The pump is then modulated by a phase modulator driven by a 1-Gb/s or 10-Gb/s pseudorandom bit sequence (PRBS) depending on the input signal modulation rate. The polarization for phase modulation is optimized by controlling PC2. The spectral characteristics of the 1-Gb/s modulated, and the 10-Gb/s modulated pumps are shown in figure 3-4. The modulated pump is directed to a high power EDFA and amplified to give an average output power up to 27 dBm. The amount of delay can be tuned continuously by adjusting output power of the high power EDFA. After amplification, the pump is launched to the SMF-33 single mode fiber through an optical circulator. By counter propagating the pump and signal pulses in the fiber that serves as slow light medium, the signal pulses are amplified by the Brillouin gain. By Kramers-Kronig relations, a group index change is associated with the Brillouin gain. Therefore, the signal pulses are delayed. The delayed signal pulses are attenuated before detecting by a fast photo-detector (3-dB bandwidth of 36 GHz) and displayed on a 50-GHz

sampling oscilloscope. The pulse delay is determined from the waveform traces displayed on the oscilloscope.

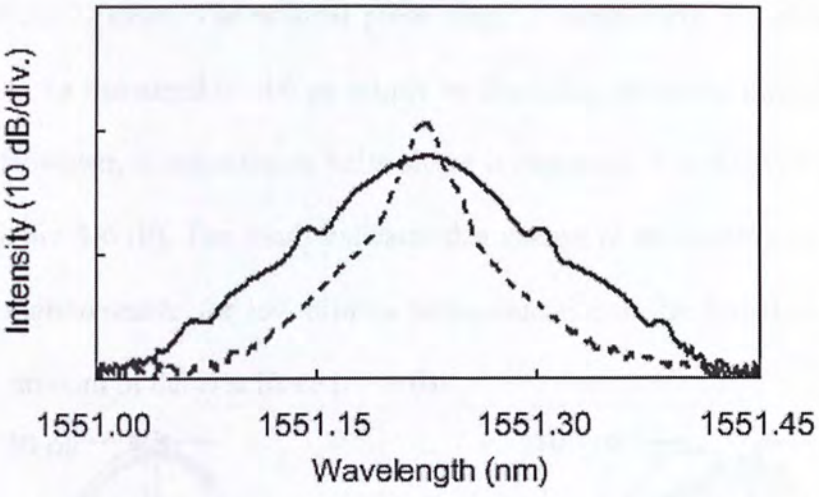

Figure 3-4: Spectrum of optical pumps. Dotted curve: phase-modulated at 1 Gb/s; (b) Solid curve: phase- modulated at 10 Gb/s

3.5 Experimental result

In the experiment, we first generate 386-ps signal pulses at 1 GHz. The waveform and spectrum of the input signal is shown in figure 3-5. The pulses are delayed using two separate sets of modulated pumps.

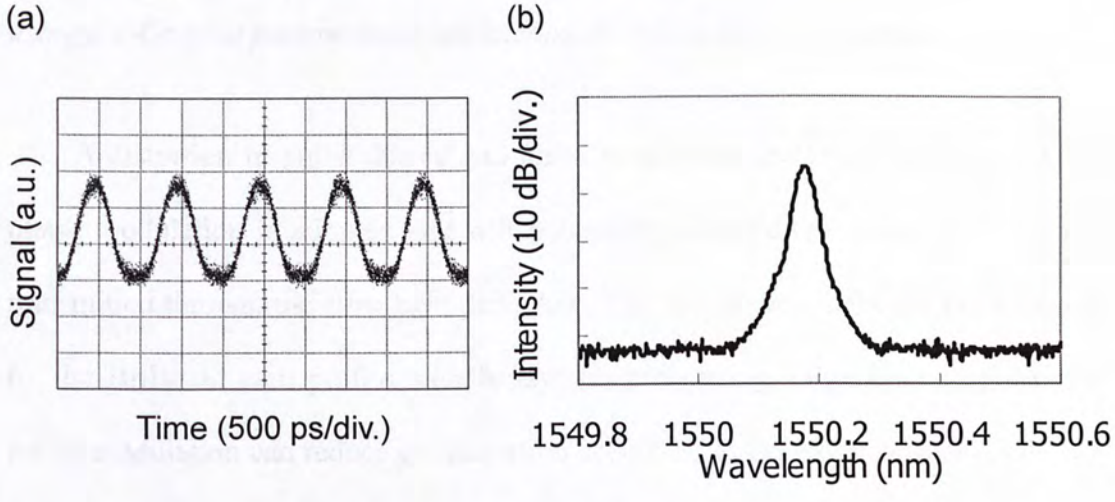

Figure 3-5: (a) Waveform of the 1 GHz input signal; (b) Spectra of the 1 GHz input signal

In figure 3-6 (a), the pulses are delayed using a phase-modulated pump at 10 Gb/s driven with a PRBS (2^{31}-1). A 30-ps delay is obtained when the average pump power is about 27 dBm. The original pulse shape is maintained. We observed that the delay can be increased to 100 ps simply by changing the pump modulation rate to 1-Gb/s. However, a distortion in pulse shape is observed. The delayed pulses are shown in figure 3-6 (b). The result indicates that excessive broadening of the pump linewidth is unfavorable for low-bit-rate communication using broad pulses as it reduces the amount of delay achieved.

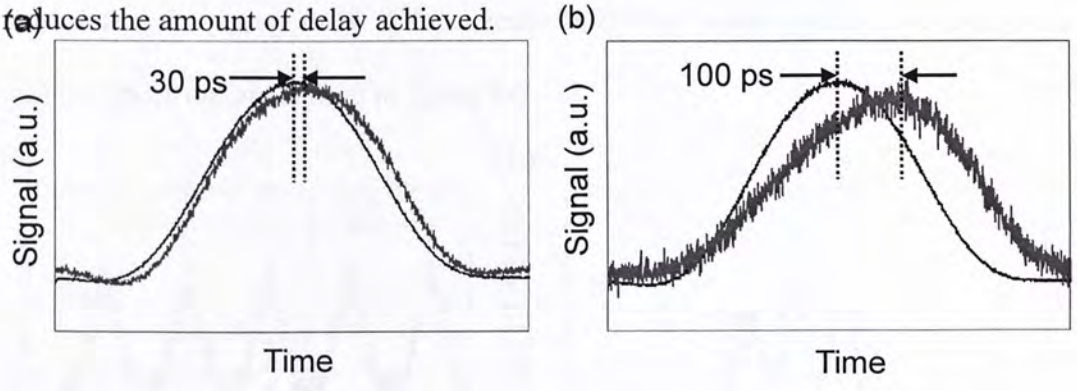

Figure 3-6: (a) Temporal profiles of the 1-GHz input pulse (blue) and the delayed pulse (violet) using a 10-Gb/s PRBS pump modulation. A 30-ps delay is obtained. (b) Temporal profiles of the 1-GHz input pulse (blue) and the delayed pulse (violet) using a 1-Gb/s bit pattern pump modulation. A 100-ps delay is obtained.

A distortion in pulse shaped and pulse broadening are observed when 1-Gb/s phase modulation is adopted and will potentially degrade the actual data that are transmitted through the slow light delay line. The distortion is believed to be caused by the Brillouin gain profile with bandwidth broadening. High bit rate (10-Gb/s) pump modulation can reduce the distortion according to the experimental result, but excessive broadening of pump linewidth reduces the amount of delay achieved. An optimum linewidth of the pump is crucial in achieving a balance between delay and

signal degradation. The signal becomes more vulnerable to distortion when the signal bandwidth is comparable to bandwidth of slow light. Therefore, higher bit rate pump modulation is flavor to signal quality. Different modulation formats exhibit different tolerance to the filtering effect induced by narrow SBS gain bandwidth. For RZ-OOK and NRZ-OOK signal, the 3-dB bandwidths of around twice the data rate are found to be optimum as described in [11]. To demonstrate the delay of the shorter pulses for high-bit-rate communication, we increase the signal modulation frequency to 10 GHz to generate 26.6-ps signal pulses. The time profile and the spectrum are shown in figure 3-7.

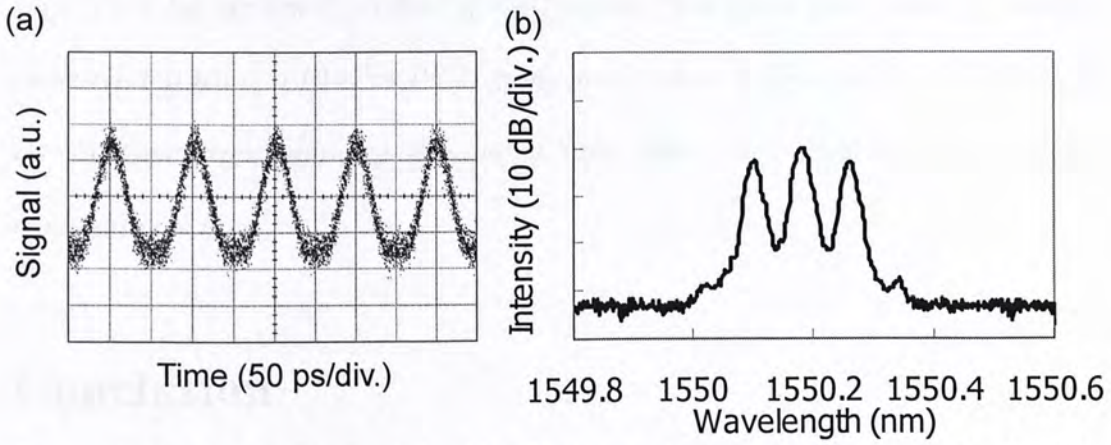

Figure 3-7: (a) Waveform of the 10 GHz input signal; (b) Spectra of the 10 GHz input signal

With a 10-Gb/s PRBS phase-modulated pump of 27 dBm average power, a delay of 10 ps is obtained. The result is shown in figure 3-8 (a). The optical pulse maintained its original shape; however, a pulse broadening of 6 ps is measured. The measured output width is 32 ps, corresponding to a broadening factor of 1.2. The pulse broadening is predicted to be reduced with higher pump modulation rate as discussed before. When a 1-Gb/s modulation is used to phase-modulate the pump, the resultant SBS gain bandwidth is insufficient to support the delay of the pulse.

Figure 3-8 (b) shows the measured output that contains only noise at the output due to narrowband filtering of signal. The result confirmed sufficient pump linewidth broadening is necessary for narrow signal pulses.

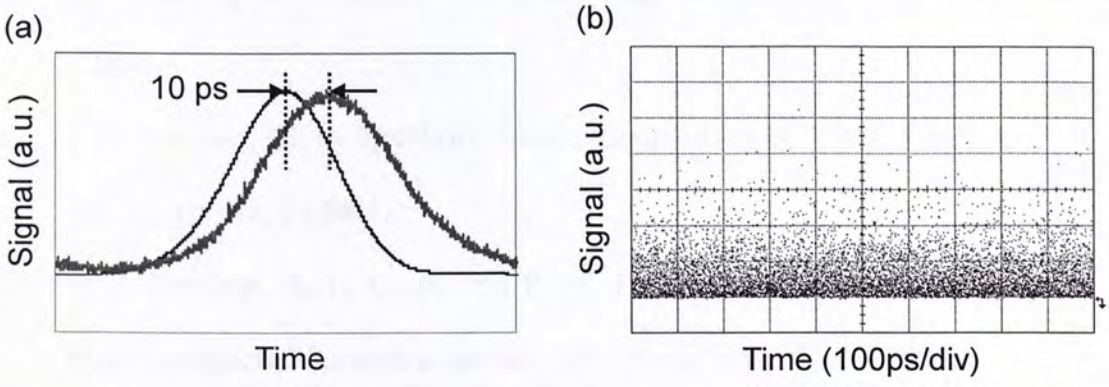

Figure 3-8 (a) Temporal profiles of the 10-GHz input pulse (blue) and the delayed pulse (violet) using a 10-Gb/s PRBS pump modulation. A 10-ps delay is obtained. (b) Oscilloscope trace showing the output noise when a 1-Gb/s bit pattern pump modulation is used.

Conclusion

We demonstrate slow light for pulses up to 10 GHz in a single mode fiber using a phase modulated pump. With an average power of 27 dBm and a 1-Gb/s pump modulation, a 386-ps pulse is delayed by 100 ps. To support the delay of shorter pulses for higher bit-rate communication, the pump is modulated at 10-Gb/s to produce a broader linewidth. A delay up to 10 ps has been achieved for 26 ps pulse. The correlation between signal pulse width and the phase modulation rate is reported.

References

[1] R. W. Boyd and D. J. Gauthier, "'Slow' and 'Fast' Light," *Progress in Optics* 43, edited by E. Wolf (Elsevier, Amsterdam, 2002), Chap. 6, pp. 497 – 530 (2002).

[2] D. J. Gauthier, "Slow light brings faster communication," Phys. World, vol. 18, vol. 12, pp. 30-32 (2005).

[3] D. J. Gauthier, A. L. Gaeta, and R. W. Boyd, "Slow Light: From basics to future prospects," Photonics Spectra, vol. 40, vol. 3, pp. 40-50 (2006).

[4] R. W. Boyd, D. J. Gauthier, and A. L. Gaeta, "Applications of slow light in telecommunications," Optics & Photonics News, vol. 17, vol. 4, pp. 19-23 (2006).

[5] Y. Okawachi, M. S. Bigelow, J. E. Sharping, Z. Zhu, A. Schweinsberg, D. J. Gauthier, R. W. Boyd, and A. L. Gaeta, "Tunable all-optical delays via Brillouin slow light in an optical fiber," Phys. Rev. Lett., vol. 94, pp. 153902 (2005).

[6] K. Y. Song, M. G. Herr´aez, and L. Th´evenaz, "Observation of pulse delaying and advancement in optical fibers using stimulated Brillouin scattering," Opt. Express, vol. 13, no. 1, pp. 82–88 (2005).

[7] J. E. Sharping, Y. Okawachi, and A. L. Gaeta, "Wide bandwidth slow light using a Raman fiber amplifier," Opt. Express, vol. 13, no. 16, pp. 6092–6098 (2005).

[8] D. Dahan and G. Eisenstein, "Tunable all optical delay via slow and fast light propagation in a Raman assisted fiber optical parametric amplifier: a route to all optical buffering," Opt. Express, vol. 13, no. 16, pp. 6234–6249 (2005).

[9] Z. Zhu, A. M. C. Dawes, and D. J. Gauthier, "12-GHz-Bandwidth SBS Slow Light in Optical Fibers", in Proc. OFC/NFOEC 2006, PDP1.

[10] M. Denariez and G. Bret, "Investigation of Rayleigh wings and Brillouin stimulated scattering in liquids,"Phys. Rev. 171, 160-171 (1968).

[11] P. J. Winzer, M. Pfennigbauer, M. M. Strasser, and W. R. Leeb, "Optimum filter bandwidths for optically preamplified NRZ receivers," J. Lightw. Techol., vol. 19, no. 9, pp. 1263-1273 (2001)

CHAPTER 4

Signal wavelength transparent SBS slow light using XGM based wavelength converter and Brillouin fiber laser

In the previous chapter, we demonstrate slow light via stimulated Brillouin scattering (SBS) using a phase-modulated pump to support slow light on high speed signal. However, the slow light via SBS requires the signal wavelength to be aligned with the Stokes shifted wavelength, therefore pump and signal wavelength alignment is required to maximize the induced time delay. In this chapter, we demonstrate a wavelength transparent stimulated Brillouin scattering (SBS) approach for slow light. Our approach makes use of a cross gain modulation (XGM) based wavelength converter and a Brillouin fiber laser. The input signal is wavelength converted to become spectrally aligned to the resonance induced by SBS. The maximum delay achieved is 26 ns with a 30 dB Brillouin gain. The delay variation is less than 0.2 ns over 40-nm wavelength detuning of the input signal.

4.1 Introduction

Tunable optical delay line is a fundamental building block for optical signal processing and buffering in a communication network. In the past few years, different techniques have been developed to realize an all-optical delay line. In particular, the slow light technique [1] has received much attention. It offers continuously tunable delay by reducing the group velocity of the signal. Slow light also increases the interaction time of light waves for use in optical sensing and nonlinear signal processing. It can be achieved in an optical fiber by stimulated Raman scattering (SRS), optical parametric amplification (OPA), and stimulated Brillouin scattering (SBS). Slow light using SBS [2][3] is particularly attractive as it requires only a relatively low pump power. Also, no phase matching is needed to achieve a large delay. The Stokes shift in SBS is determined by the fiber waveguide structure and the doping level of germanium inside the fiber core. To achieve SBS slow light, the input signal must be spectrally aligned to the SBS induced resonance. The amount of delay is tuned by adjusting the Brillouin gain. The intrinsic SBS gain bandwidth is around 30 MHz in a conventional single mode fiber, thus limiting the input data rate to the megabit range. The gain bandwidth can be broadened [4][5][6] to support gigabit data rate in an optical communication network. Recently, an operation bandwidth of up to 25 GHz has been reported [7]. Another major challenge for SBS slow light is that the delay can be obtained only when the signal wavelength falls within the bandwidth of resonance. A precise pump wavelength is required. The input signal wavelength is fixed unless a tunable pump laser with a very fine tuning resolution and high wavelength stability is used.

In this chapter, we propose and demonstrate a novel SBS slow light architecture for tunable delay. Our approach offers a wavelength transparent

operation to the input signal. The signal wavelength is converted to become spectrally aligned to the SBS induced resonance regardless of its original wavelength. The wavelength transparency is achieved with the use of a cross-gain modulation (XGM) based wavelength converter and a Brillouin fiber laser. The wavelength transparent range is found to be over 40 nm. Our approach eliminates the need of precise pump tuning and supports slow light with different signal wavelengths without changing the pump wavelength. Hence, it offers a practical and cost effective solution for the use in optical communication network.

4.2 Brillouin fiber laser and XGM wavelength converter

The Brillouin gain in the optical fiber can be used to make Brillouin fiber lasers by placing the fiber inside a cavity. Both the ring cavity and the Fabry-Perot cavity have been demonstrated for lasing. The Brillouin threshold is found to occur at a critical power P_{cr} obtained from the relation [8],

$$\frac{g_b P_{cr} L_{eff}}{A_{eff}} \approx 21 \tag{4.1}$$

where g_b is the peak value of the Brillouin gain, L_{eff} is the effective length of the optical fiber and A_{eff} is the effective area of the optical fiber. For Brillouin fiber laser, the threshold pump power required for oscillations is considerably reduced because of the feedback provided by the cavity. Typically the factor 21 is replaced by a number in the range 0.1-1 depending on the coupling losses. The Brillouin fiber laser adopted in our setup is built by a 600-m fiber ring cavity shown schematically in figure 4-1. A DFB pump laser (λ_p) is routed to the fiber ring cavity via an optical

circulator. The pump is scattered to generate the Stokes wave (λ_B) in the SMF-33 standard single mode fiber, which is counter-propagating with the pump inside the fiber cavity. The Stokes wave is further amplified in the single mode fiber in another round trip. A coupler is used to branch out part of the Stokes wave power as the output. The output spectrum of the Brillouin fiber laser and pump laser is shown in figure 4-2.

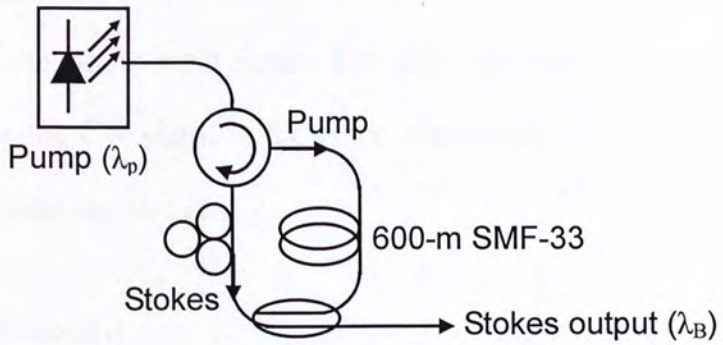

Figure 4-1: Schematic illustration of a Brillouin fiber laser built by a 600-m fiber ring cavity.

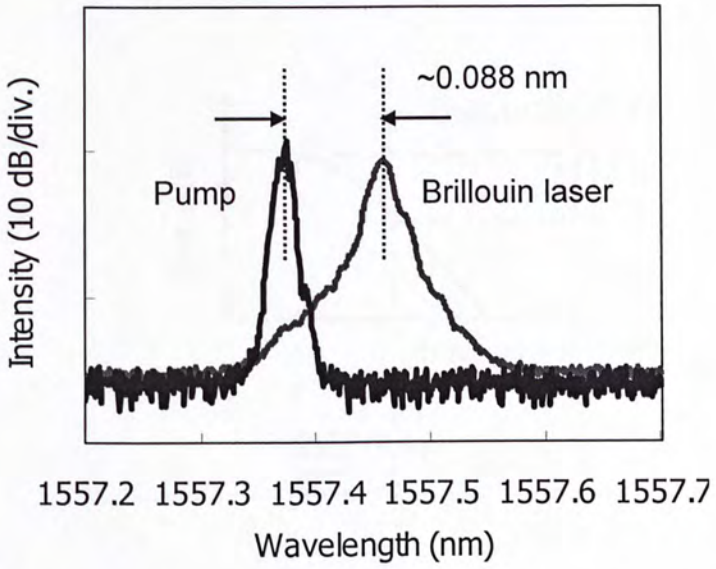

Figure 4-2: Optical spectrum of pump laser and output spectrum of Brillouin fiber laser.

All-optical wavelength converter can be built by using cross gain modulation (XGM) in an SOA [9]. The basic principle of a XGM wavelength converter is illustrated in figure 4-3. An intensity modulated signal (λ_1) is injected into a SOA, along with a continuous wave (CW) probe signal (λ_2), as shown in figure 4-3(a). The power level of the "ones" of input signal is sufficiently high to compress the gain of the SOA, as shown in the schematic saturation characteristic in figure 4-3(b). This gain compression results from the carrier depletion caused by stimulated emission in the presence of the strong input signal. The gain modulation caused by the input signal modulates the CW signal at the probe wavelength, thus an inverted data is obtained at the probe wavelength.

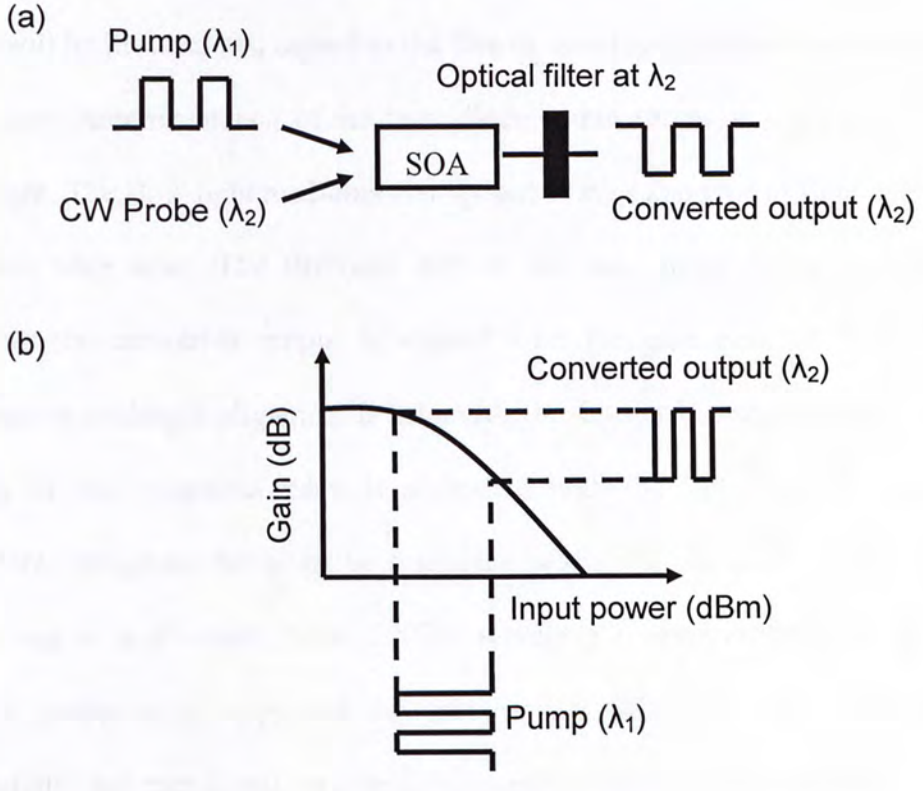

Figure 4-3: Principle of operation of XGM based wavelength converter

4.3 Operating principle

Figure 4-4 shows the schematic illustration of our wavelength transparent SBS slow light approach. A laser diode is used simultaneously as the pump for a Brillouin fiber laser and the pump for SBS slow light. The laser output is divided into two branches. The first branch serves as the pump in a Brillouin fiber laser that downshifts the frequency of the laser diode by an amount equal to the Stokes shift of the optical fiber used in the cavity. The Brillouin laser output is then used as the probe light of a wavelength converter. The signal to be delayed is directed to the wavelength converter. The wavelength converter used is based on cross-gain modulation in an SOA. Due to gain competition, the information carried at the signal will be inverted and copied to the Stokes wavelength defined by the Brillouin fiber laser. Another branch of the laser diode output serves as the pump for SBS slow light. The slow light medium is composed of the same type of fiber used in the Brillouin fiber laser. The Brillouin shift of the two optical fibers are identical, therefore the converted output is aligned with the gain peak of SBS. Hence, automatic wavelength alignment is achieved. By Kramer-Kronigs relations, a rapid change of the refractive index is associated with the SBS induced resonance. Therefore, the group index at the resonance is sharply increased. A delay of the optical signal is obtained. Since a XGM wavelength converter is used, the signal will be converted to align with the gain peak of SBS regardless of its original wavelength, and thus signal wavelength transparent operation is achieved.

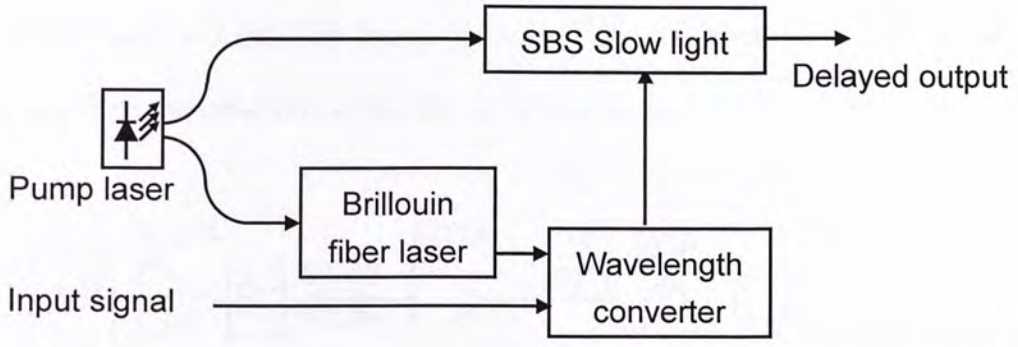

Figure 4-4: Schematic illustration wavelength transparent SBS slow approach

4.4 Experimental setup and results

The experimental setup is shown in figure 4-5. The output of a 1553.920-nm laser diode is amplified by an EDFA to produce an average power of 15 dBm. An optical bandpass filter is used to filter out the amplified spontaneous emission noise after the amplification. The pump is then split into two branches with a 3-dB coupler. One branch is directed to a Brillouin fiber laser constructed with a 600-m SMF-33 standard single mode fiber. The Stokes shift of the fiber is ~10.83 GHz. The measured Brillouin gain spectrum is shown in figure 4-6. Hence, a down-shifted Stokes wave is generated by the fiber laser as the probe light. The wavelength of the probe is about 1554.008 nm. In our experiment, the signal pulses to be delayed are generated by externally modulating a tunable laser with a 10-MHz sinusoidal RF signal. A higher modulation frequency can be used if the pump linewidth is broadened to increase the gain bandwidth by SBS. The electro-optic modulator is biased to generate a 30-ns (FWHM) inverted signal pulse as shown in figure 4-7 (a). The signal pulses are routed to the semiconductor optical amplifier (SOA) via an optical circulator (OC2). The pulses and the Brillouin fiber laser probe light counter-propagate in the SOA. Non-inverted signal pulses are thus

generated on the probe wavelength by XGM wavelength conversion. The result is shown in figure 4-7 (b). The intensity noise of the converted pulse is believed to originate from the instability of the Brillouin fiber laser.

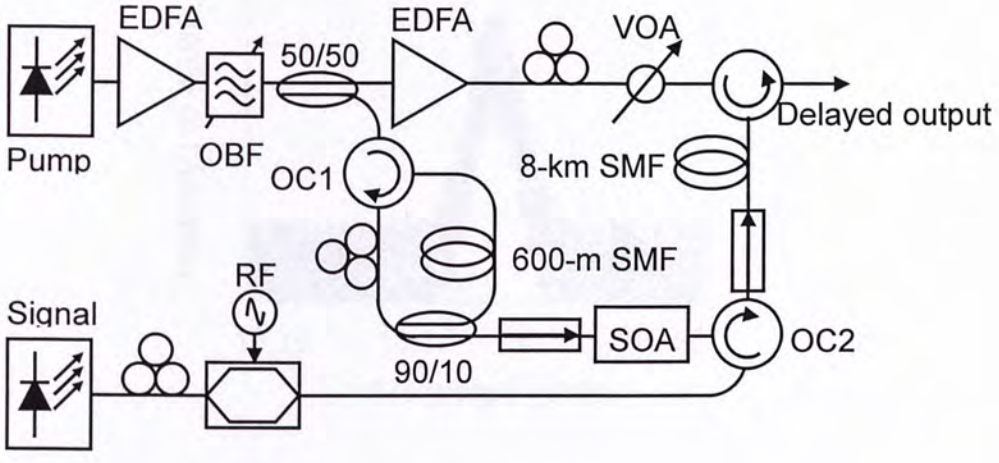

Figure 4-5: Experimental setup of the slow light approach. LD: laser diode; TL: tunable laser; EDFA: erbium doped fiber amplifier; OBPF: optical bandpass filter; SOA: semiconductor optical amplifier; OC1, OC2, and OC3: optical circulator; SMF: single mode fiber; EOM: electro-optic modulator; VOA: variable optical attenuator.

The other branch of the pump is amplified with a high power EDFA to produce a 30 dBm average output. A variable optical attenuator is used to control the pump power. The amplified pump is then routed via another optical circulator (OC3) to an 8-km SMF-33 single mode fiber that serves as the slow light medium. The Stokes shift in the slow light medium is the same as the Stokes shift in the Brillouin fiber laser. Hence, the fiber laser output, now carrying the signal pulses, is aligned exactly with the Brillouin resonance induced in the slow light medium. Therefore allows signal wavelength transparent operation. By counter-propagating the pump and the

converted signal in the fiber, the converted signal is simultaneously amplified and delayed. With adjustment of the pump power, different amounts of Brillouin gain and delay are achieved.

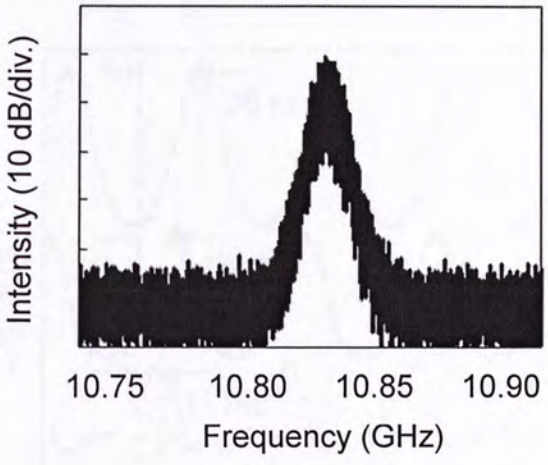

Figure 4-6: Measured Brillouin spectrum of SMF-33 standard single mode fiber

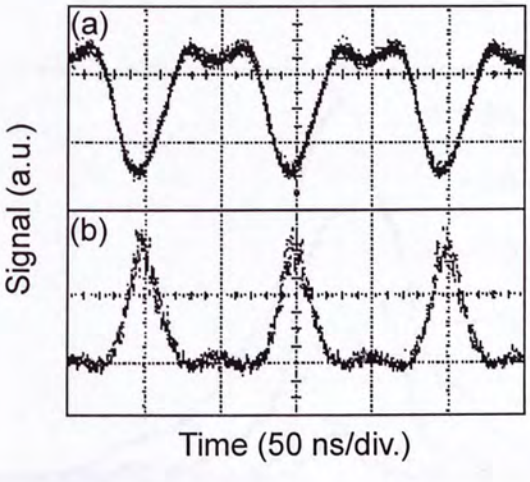

Figure 4-7: Time profiles of (a) Inverted input pulses at 1548.440 nm, (b) Non-inverted output pulses at 1554.008 nm after XGM wavelength conversion.

By controlling the pump power, a continuously tunable delay up to 26 ns has been achieved. The delay increases from 11 to 19 and 26 ps when the gain is increased from 10 to 20 and 30 dB. Figure 4-8 (a) and (b) depict the temporal profiles and the spectra measured at different levels of the Brillouin gain. The

achieved pulse delay scales linearly with the optical gain at 1.15 ns/dB. The result is shown in figure 4-9. The result confirms that the induced time delay can be tuned continuously.

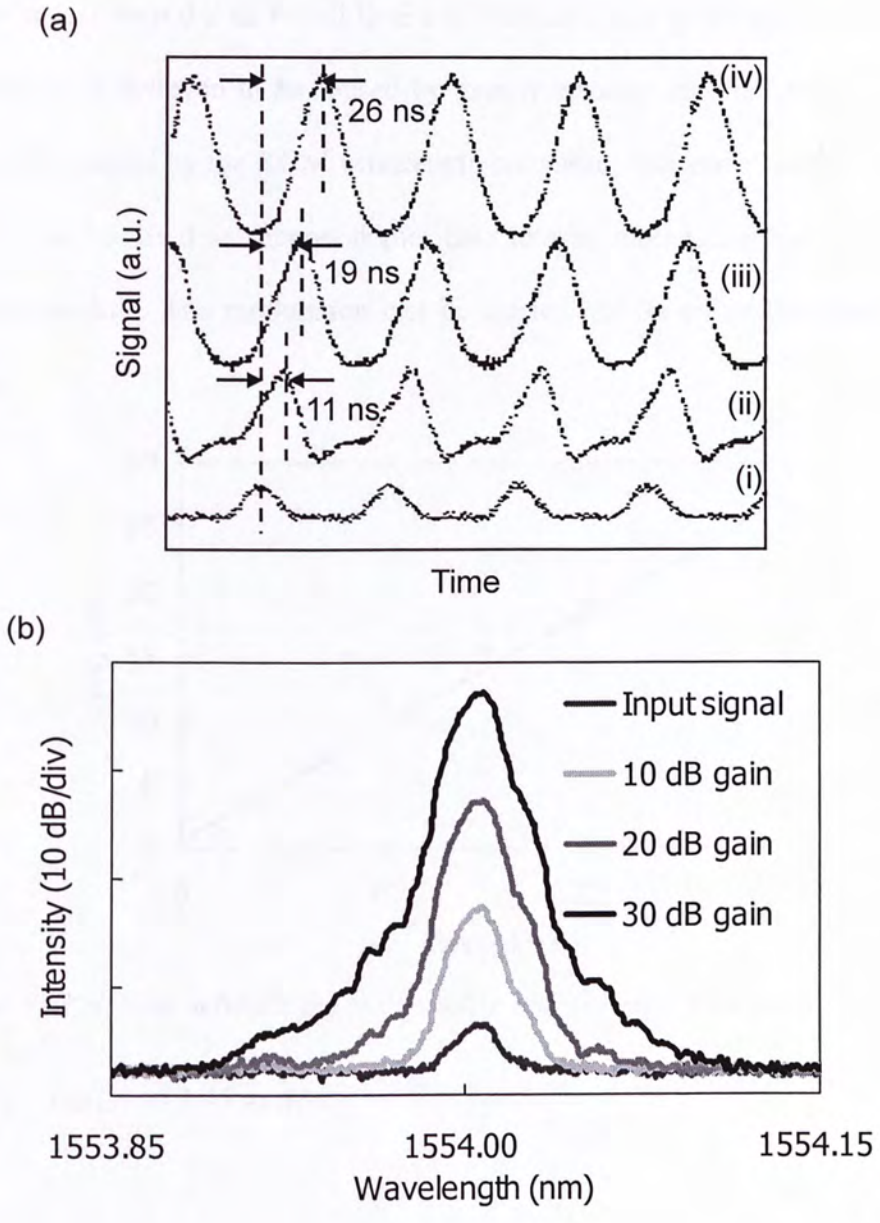

Figure 4-8: (a) Time profiles of (i) input signal, (ii) – (iv) delayed signals with different Brillouin gains at 10 dB, 20 dB, and 30 dB. (b) Optical spectra of the input signal and the delayed signals at different Brillouin gains.

To study the wavelength transparent characteristic of our approach, the tunable laser is tuned over 40 nm from 1540 to 1580 nm. The operating range is limited by the conversion bandwidth of the XGM based wavelength converter. The delay variation is less than 0.2 ns for all levels of Brillouin gain as shown in figure 4-10. The variation is believed to be caused by gain fluctuation and the slight change in pulse profile caused by the XGM wavelength converter. The wavelength transparent setup can be modified to support higher data rate by modulating the pump in the slow light module. The modulation can be carried out on either the phase or the intensity.

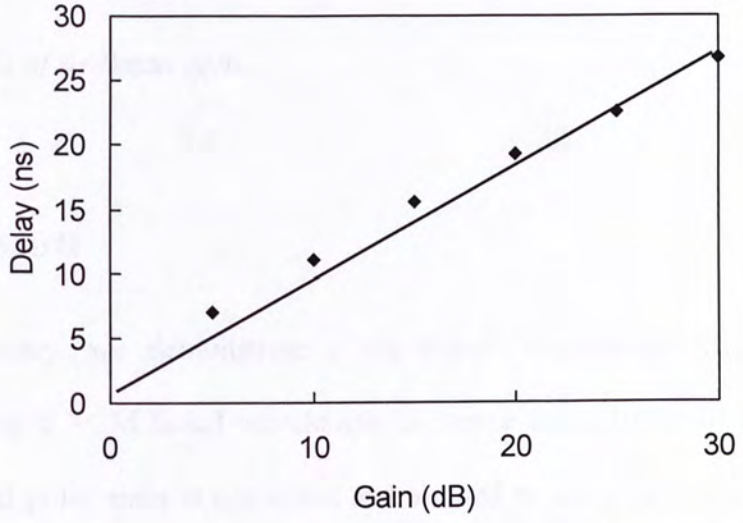

Figure 4-9: Relation between the pulse delay and the Brillouin gain. The linear plot shows a delay of 1.15 ns/dB.

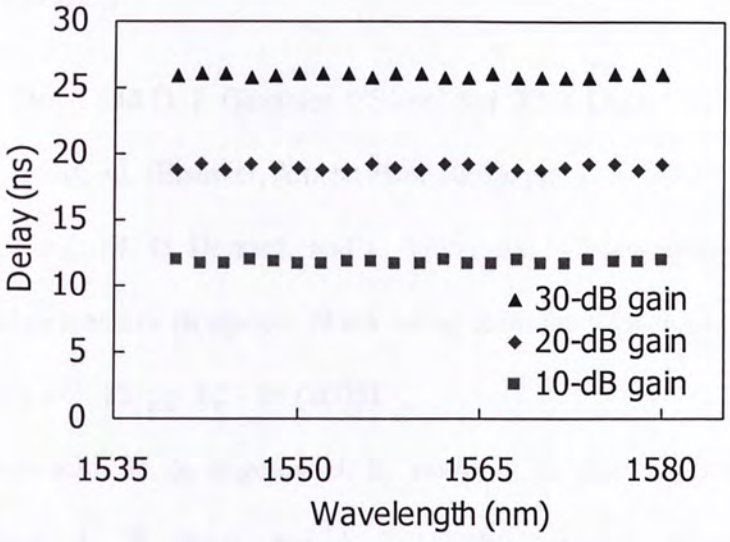

Figure 4-10: Measured pulse delay as a function of input signal wavelength at different levels of Brillouin gain.

Conclusion

In summary, we demonstrate a wavelength transparent SBS slow light approach using a XGM based wavelength converter and a Brillouin fiber laser. A 30-ns inverted pulse train is converted and aligned to the SBS induced resonance regardless of its original wavelength. Using a high power EDFA, continuously tunable delay up to 26 ns has been achieved. The wavelength transparent characteristic is verified by detuning the input signal wavelength from 1540 nm to 1580 nm. The variation of the delay is less than 0.2 ns. The approach offers a practical means to perform buffering or synchronizing operation in WDM optical communication networks.

References

[1] R. W. Boyd and D. J. Gauthier, "'Slow' and 'Fast' Light," in Progress in Optics 43, E. Wolf, ed. (Elsevier, Amsterdam, 2002), pp. 497 – 530

[2] K. Y. Song, M. G. Herraez, and L. Thevenaz, "Observation of pulse delaying and advancement in optical fibers using stimulated Brillouin scattering," Opt. Express vol. 13, pp. 82 - 88 (2005).

[3] Y. Okawachi, M. S. Bigelow, J. E. Sharping, Z. Zhu, A. Schweinsberg, D. J. Gauthier, R. W. Boyd, and A. L. Gaeta, "Tunable all-optical delays via Brillouin slow light in an optical fiber," Phys. Rev. Lett. vol. 94, no. 15, 153902 (2005).

[4] M. G. Herraez, K. Y. Song, and L. Thevenaz, "Arbitrary-bandwidth Brillouin slow light in optical fibers," Opt. Express, vol. 14, pp. 1395- 1400 (2006).

[5] Z. Zhu, A. M. C. Dawes, D. J. Gauthier, L. Zhang, and A. E. Willner, "Broadband SBS Slow Light in an Optical Fiber," J. Lightwave Technol., vol.25, 201-206 (2007).

[6] B. Zhang, L. Yan, I. Fazal, L. Zhang, A. E. Willner, Z. Zhu, and D. J. Gauthier, "Slow light on Gbit/s differential-phase-shift-keying signals," Opt. Express, vol. 15, 1878-1883 (2007).

[7] K. Y. Song and K. Hotate, "25 GHz bandwidth Brillouin slow light in optical fibers," Opt. Lett. 32, 217-219 (2007).

[8] R. G. Smith, " Optical power handling capacity of low loss optical fiber as determined by stimulated Raman and Brillouin scattering," Appl. Opt., vol. 11, 2489-2494 (1972).

[9] T. Durhuus, B. Mikkelsen, C. Joergensen, S. L. Danielsen and K. E. Stubkjaer, "All optical wavelength conversion by semiconductor optical amplifier," J. Lightw. Technol. vol. 14, pp. 942-954 (1996).

CHAPTER 5

All-optical tunable delay line for channel selection in a 40-Gb/s optical time division multiplexing system

In chapter 3, we introduce a wideband all-optical tunable delay line using a phase modulated pump via stimulated Brillouin scattering (SBS). The pump linewidth is broadened to support 10-Gb/s data. However, the delay-bandwidth product restricts the maximum amount of delay at high bit rate and limits its application in optical communication networks. In this chapter, we propose another type of all-optical tunable delay line using four-wave mixing (FWM) wavelength conversion together with group velocity dispersion (GVD). There is no inherent trade-off between the signal bandwidth and the amount of tunable delay. To show the applications of our proposed tunable delay line, a channel selectable 40-Gb/s OTDM signal demultiplexing scheme is demonstrated using our tunable delay line. The demultiplexing is performed by optical gating in an electro-absorption modulator (EAM) via cross absorption modulation (XAM). By tuning the delay of the optical clock, fast channel selection can be achieved.

5.1 Introduction

Tunable optical delay line is a fundamental building block for signal processing in an optical communication network. The delay can be used for optical buffering, data packet synchronization, and bit-level synchronization [1]. Various techniques have been demonstrated to achieve a tunable delay. Examples are the switching among a discrete set of optical paths [2], slow light in an optical fiber [3][4], and wavelength conversion with group velocity dispersion [5][6][7].

The demand on the bandwidth requirement of internet is increasing dramatically due to the rapid growth in broadband multimedia services [8]. In modern optical communication networks, the transmission capacity can be expanded by increasing the number of wavelength channels or by increasing the bit-rate in each channel. Wavelength division multiplexing (WDM) system is employed in long-haul communication network to increase the channel number by transmitting different channels via different wavelengths on the same fiber simultaneously. The WDM system can increase the transmission capacity without increasing the speed of each channel. Time division multiplexing (TDM) system is employed to increase the per channel bit rate by allocating a specific time-slot to each information channel in a continuous bit-stream. Intense efforts in the demonstration and deployment of this high capacity WDM/TDM networks are in progress [9][10]. A transmission system employing OTDM is an attractive solution to future high bit rate TDM optical communication system [11]. However, electronic circuits are creating a bottleneck on the operation as high speed electronics are limited up to ~ 50 GHz and are very expensive. Recently, many researches are targeting on all-optical signal processing to overcome the electronic speed limit. All-optical signal processing provides a potentially high speed and relatively inexpensive method for the OTDM optical

networks.

All-optical demultiplexing of OTDM system can be achieved using the time gating technique. To select different channels, the time delay of the incoming gating signal should be varied. An all-optical tunable delay line offers optically controlled and fast tuning speed for the demultiplexing. In this chapter, we present a 40-Gb/s to 10-Gb/s optical time division multiplexing (OTDM) demultiplexer using an optical delay line. The optical delay line is constructed by four-wave mixing wavelength conversion and wavelength-dependent group delay in a chirped fiber Bragg grating. Unlike the stimulated Brillouin scattering slow light technique, there is no inherent trade-off between the signal bandwidth and the amount of tunable delay. Also, the delayed pulses are not distorted or broadened. The demultiplexing is performed by optical gating in an electro-absorption modulator (EAM) via cross absorption modulation. By tuning the delay of the optical clock, fast channel selection can be achieved.

5.2 Principle of four-wave mixing

The origin of parametric processes lies in the nonlinear response of bound electrons of a material to an applied optical field. More specifically, the polarization induced in the medium is nonlinear to the applied field and is governed by the nonlinear susceptibilities. The parametric processes are dominated by second-order or third order parametric processes depending on whether second-order or third order susceptibility is involved. It is well known that the third-order parametric processes are more important in a silica fiber owing to inversion symmetry. The third-order parametric processes involve in general the interaction among four optical waves and include the phenomena such as third-harmonic generation,

four-wave mixing (FWM), and parametric amplification. Four-wave mixing is being studied extensively since it is an efficient way for the generation of new waves. In the case of four-wave mixing, phase matching is required. In the context of quantum mechanics, four-wave mixing occurs when photons from one or more waves are annihilated and new photons are created at different frequencies such that the net energy and momentum are conserved during the parametric interaction. A schematic illustration of typical four-wave mixing is shown in figure 5-1. Consider four optical waves oscillating at frequencies ω_S, ω_P, ω_3, ω_4, phase matching should be achieved at $\omega_4 = 2\omega_S - \omega_P$ and $\omega_3 = 2\omega_P - \omega_S$. The electric field of the two newly generated waves can be written as,

$$E_3 = (\vec{E}_{P1} \cdot \vec{E}_S^{\,*}) E_{P1} \gamma(\omega_{P1} - \omega_S) \exp[i(\omega_3 t + 2\phi_{P1} - \phi_S)] \tag{5.1}$$

$$E_4 = (\vec{E}_S \cdot \vec{E}_{P1}^{\,*}) E_S \gamma(\omega_S - \omega_{P1}) \exp[i(\omega_4 t + 2\phi_S - \phi_{P1})] \tag{5.2}$$

where E is the electric field of the wave, φ is the phase of the wave, and γ is the nonlinear coefficient. Note that the amplitude information and the phase of the signal is transferred to the two newly generated wave at ω_3. Therefore wavelength conversion can be achieved using FWM.

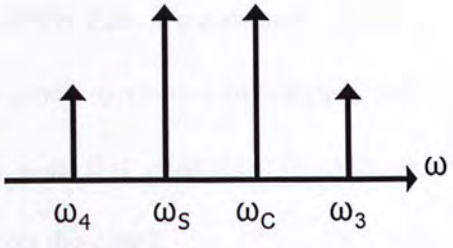

Figure 5-1: Schematic illustration of different components in FWM

5.3 Channel selection in an OTDM system

The schematic of our channel selectable OTDM system is shown in figure 5-2. The demultiplexing is based on an optical gating device built by an electro-absorption modulator (EAM). The modulator is reversely biased with an electric field. By applying an optical clock with at the baseband frequency, the clock will gives rise to a screening of the applied electric field and significantly decrease the absorption and create a transmission window. The EAM will work as an optical gate that opens periodically at the baseband frequency. The process of optically modulating the absorption is described as cross-absorption modulation (XAM). By launching the OTDM signal to the optical gate simultaneously, the OTDM signal is demultiplexed to the baseband frequency. The tunable delay line is achieved via FWM wavelength conversion in a 64-m highly nonlinear dispersion flattened photonic crystal fiber (PCF) [12] followed by chromatic dispersion. The PCF exhibits a large nonlinear coefficient at 1550 nm. Thus a 64-m fiber is sufficient to introduce FWM. The short length of fiber also leads to a large stimulated Brillouin scattering (SBS) threshold. The 3-dB conversion bandwidth of 16 nm can be achieved with the PCF. The tunable delay is produced by feeding the wavelength-converted output to a dispersive fiber medium. With the use of a chirped fiber Bragg grating (CFBG), a continuously tunable delay can be achieved by changing the wavelength of the converted output. Using an all-optical tunable delay line, the time delay on the clock can be tuned continuously. Synchronization between clock and OTDM signal and fast channel selection can be achieved by simply controlling the time delay on the clock.

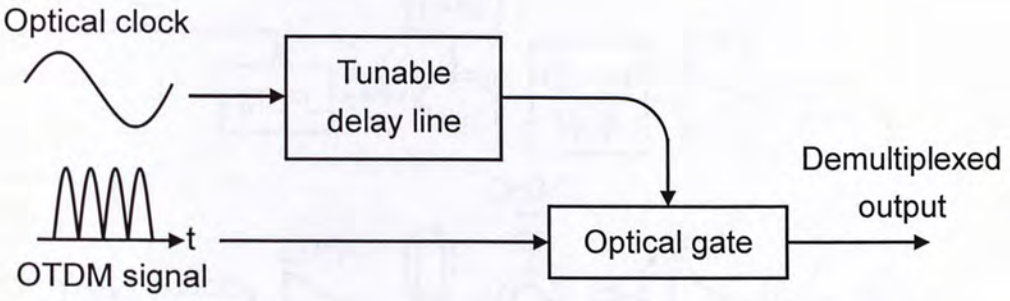

Figure 5-2: Schematic of tunable delay line for channel selection in OTDM system

5.4 Experimental setup

Figure 5-3 shows the experimental setup of the channel selectable OTDM demultiplexing. A 10-GHz mode-locked fiber laser is externally modulated by an electro-optic modulator driven by a 10-Gb/s 2^{31-1} pseudorandom bit sequence (PRBS) to generate10-Gb/s RZ-OOK signal. The output is then multiplexed using a set of 10-Gb/s to 40-Gb/s OTDM bit rate multiplier to produce a 40-Gb/s OTDM signal. The signal is amplified, directed to an optical isolator, and launched to an electro-absorption modulator (EAM). A 1551.5-nm electro-absorption modulated laser (EML) is driven at 10 GHz to produce an optical clock for demultiplexing in our experiment. The clock has a pulse width of 22 ps. To achieve high-speed channel selection and synchronization between the clock and the OTDM signal, a tunable optical delay line is built by four-wave mixing wavelength conversion followed by wavelength-dependent group delay. A CW tunable laser (TL) is used as the pump and is combined with the optical clock through a 3-dB coupler. The polarization of the TL is adjusted by a polarization controller to optimize the wavelength conversion efficiency.

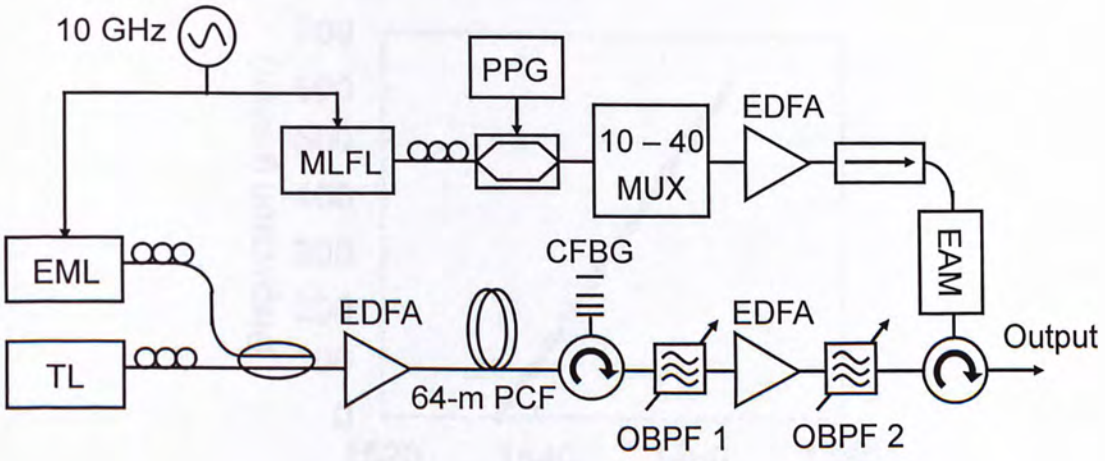

Figure 5-3: Experimental setup of 40-Gb/s demultiplexer. EML: electro-absorption modulated laser; TL: tunable laser; EDFA: erbium doped fiber amplifier; PCF: photonic crystal fiber; CFBG: chirped fiber Bragg grating; OBPF1 and OBPF2: optical bandpass filter; MLFL: mode-locked fiber laser; PPG: pulse pattern generator; 10-40 MUX: 10-Gb/s to 40-Gb/s bit rate multiplier; EAM: electro-absorption modulator

The combined output is amplified to produce an average output power of 17 dBm and is launched into a 64-m dispersion flattened (dispersion slope ~10^{-3} $pskm^{-1}nm^{-2}$), highly nonlinear (γ =11.2 $W^{-1}km^{-1}$) photonic crystal fiber (PCF) to introduce four-wave mixing. The four-wave mixing output is routed to a linearly chirped fiber Bragg grating (CFBG) through an optical circulator. The dispersion of the CFBG is measured to be 20 ps/nm. The dispersion, transmission, and reflection characteristic of the CFBG are shown in figure 5-4.

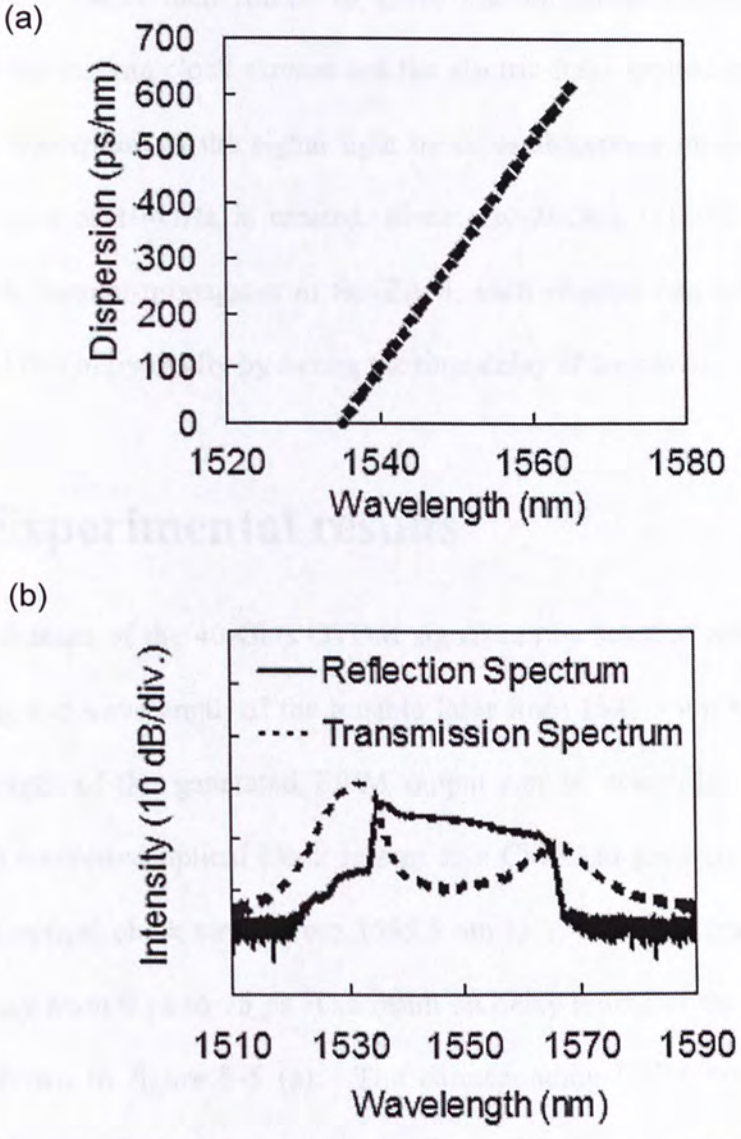

Figure 5-4: (a) Dispersion characteristic of the CFBG; (b) Reflection and transmission spectrum of the CFBG.

Different time delays are obtained by tuning the wavelength of the tunable laser. The residual pump power is blocked by a Gaussian-shaped optical bandpass filter (OBPF 1) with a 3-dB bandwidth of 0.5 nm. The delayed optical clock is then directed to another EDFA and filter by another Gaussian-shaped optical bandpass filter (OBPF2, 3-dB bandwidth 0.4 nm) to remove the amplified spontaneous emission noise (ASE) introduced. The average power of the clock is 14 dBm after

OBPF2. The clock is then routed to EAM via an optical circulator. The high intensity of the income clock screens out the electric-field applied to the EAM and reduces the absorption of the signal light by cross-absorption modulation (XAM). An optical gate at 10-GHz is created. Since the 40-Gb/s OTDM signal and the optical clock counter-propagates in the EAM, each channel can be demultiplexed down to 10 Gb/s individually by tuning the time delay of the clock.

5.5 Experimental results

Each channel of the 40-Gb/s OTDM signal can be selected and demultiplexed by adjusting the wavelength of the tunable laser from 1548.5 nm to 1550.375 nm, the wavelength of the generated FWM output can be controlled. By FWM, the wavelength converted optical clock is sent to a CFBG to generate different delay. The output optical clock varies from 1545.5 nm to 1549.25 nm corresponding to a relative delay from 0 ps to 75 ps. The result on delay tuning of the clock from 0 to 75 ps is shown in figure 5-5 (a). The corresponding FWM optical spectra are measured after the PCF and are shown in figure 5-5 (b). It is worth noting that the achievable delay can be over 75 ps, the maximum amount needed for channel selection in 40-Gb/s OTDM demultiplexing. Using XAM, each channel of the 40-Gb/s OTDM signal can be selected by changing the time delay of the optical clock. The demultiplexed channel is detected by a 36 GHz photo-detector and displayed on a 50 GHz sampling oscilloscope. The eye diagrams of the four demultiplexed channels are shown in figure 5-6. A clear and open eye can be observed in each channel after demultiplexing. Since the pulse width of the clock generated by the EML is approximately 22 ps (FWHM), the gating window of XAM is not narrow enough to completely suppress the signal in the other channels. Thus,

some ripples are observed in the measured eye diagrams. The result can be improved by using an optical clock with shorter pulses.

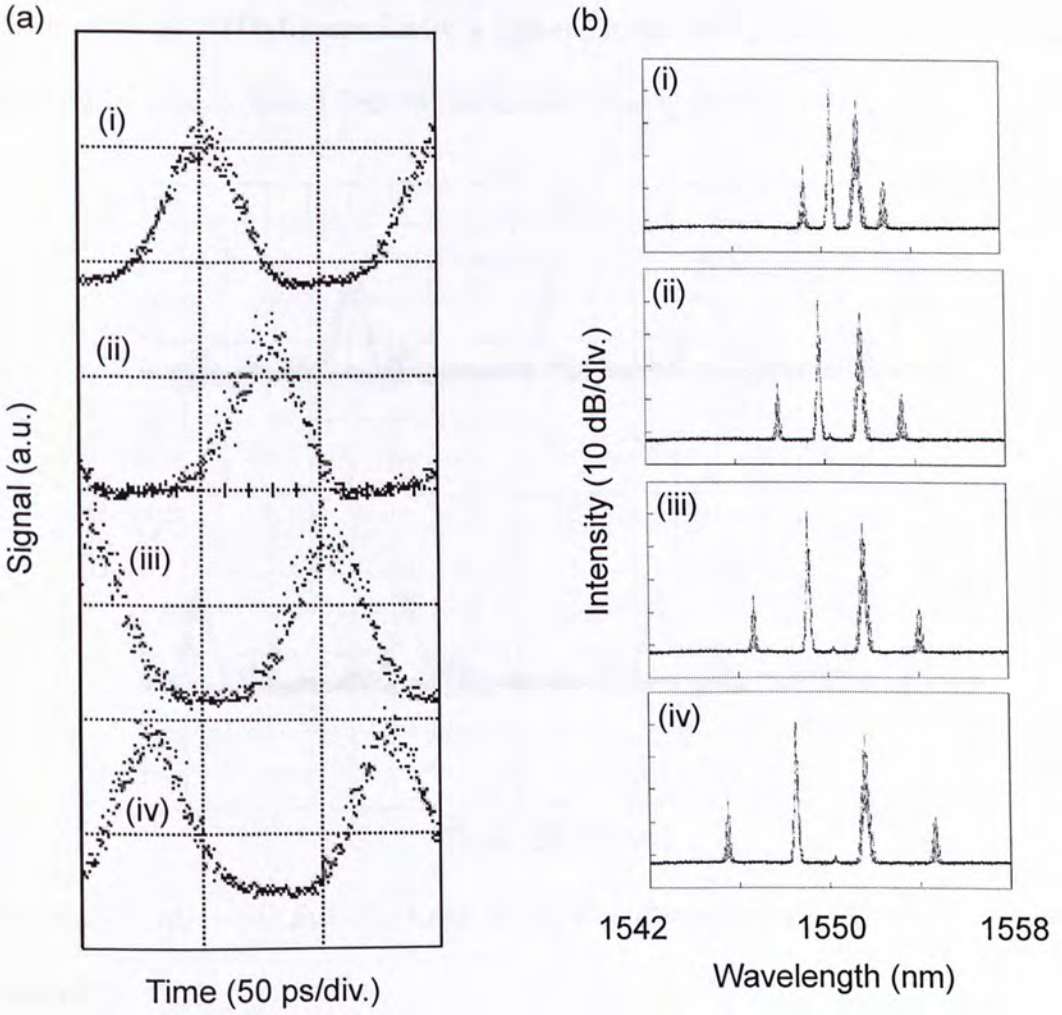

Figure 5-5: (a) Profiles of the optical clock at different time delays and (b) corresponding FWM optical spectra. The relative delays are (i) 0 ps, (ii) 25 ps, (iii) 50 ps, (iv) 75 ps.

To quantify the performance of the OTDM demultiplexer using tunable delay, BER measurements are carried out on each channel. The result is shown in Figure 5-7. The B2B case is measured before multiplexing. The power penalties of the four channels after multiplexing and demultiplexing are less than 4 dB at a BER of 10^{-9}. The signal degradation is caused by amplified spontaneous noise in the EDFAs and

the reduction in extinction ratio of the signal after the XAM process. Due to the fast response of FWM in the PCF, the setup is potentially upgradeable to support channel selection in an OTDM system with a higher bit rate using a high speed EAM or nonlinearities in an optical fiber for the demultiplexing process.

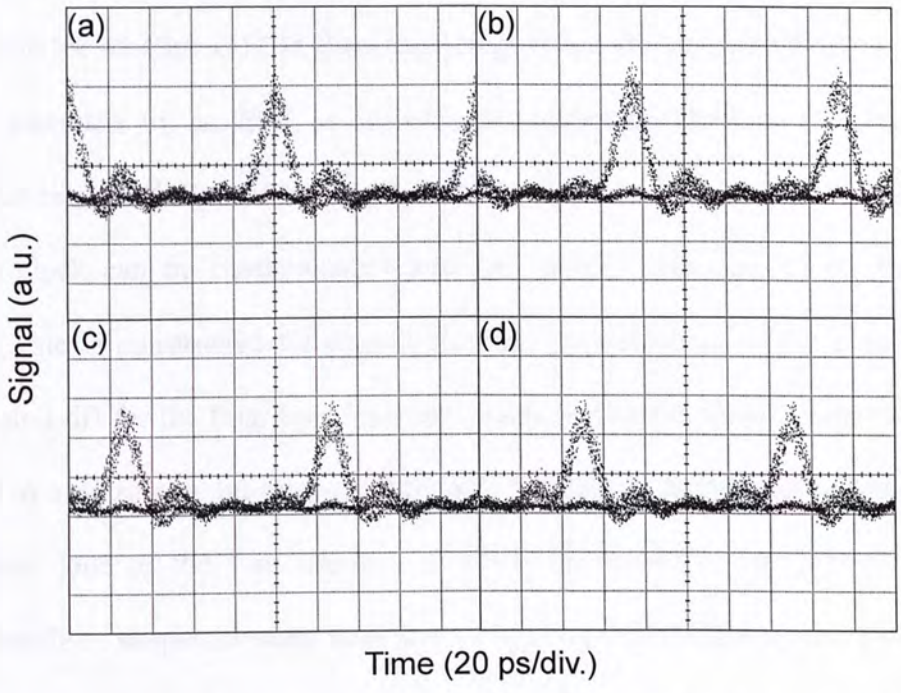

Figure 5-6: (a) – (d) Eye diagrams of 10-Gb/s demultiplexed signals at the four channels

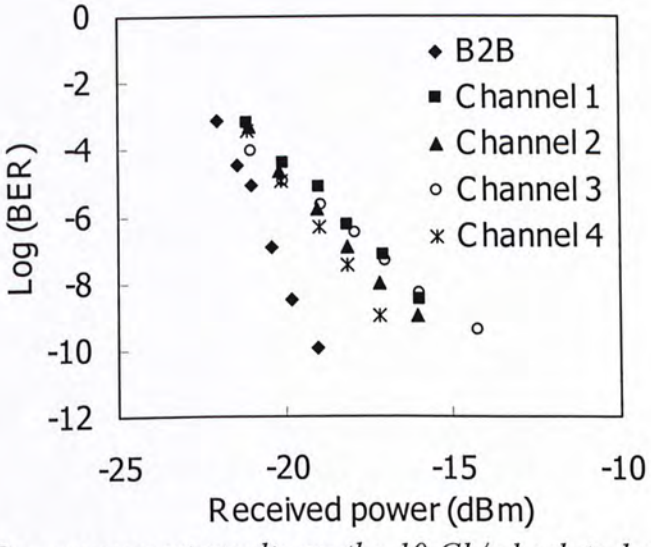

Figure 5-7: BER measurement results on the 10-Gb/s back to back signal and the four demultiplexed channels.

Conclusion

Using four-wave mixing wavelength conversion in a highly nonlinear dispersion flattened photonic crystal fiber and chromatic dispersion in a linearly chirped fiber Bragg grating, we have experimentally demonstrated an all-optical delay line for 40-Gb/s OTDM demultiplexing. Using FWM in the PCF, the optical clock generated by an EML is wavelength converted. The converted output is launched into the CFBG with a dispersion of 20 ps/nm. The delay of the incoming optical clock can be continuously tuned for channel selection. Using EAM, an optical gate is constructed for demultiplexing. The measured power penalties are less than 4 dB for the four demultiplexed channels. Our all-optical delay scheme is useful in realizing a bit-rate variable and fast-tuned demultiplexer for OTDM networks. Due to the fast response of FWM in the PCF, our scheme can be upgradeable to support channel selection for high bit rate OTDM system (>40 Gb/s) using a high speed EAM or nonlinearities in an optical fiber for the demultiplexing.

References

[1] B. Zhang, L. Zhang, L. -S. Yan, I. Fazal, J. -Y. Yang, and A. E. Willner, "Continuously-tunable, bit-rate variable OTDM using broadband SBS slow-light delay line," Opt. Express, vol. 15, 8317-8322 (2007).

[2] Y. Liu, M. T. Hill, N. Calabretta, H. de Waardt, G. D. Khoe, and H. J. S. Dorren, "All-optical buffering in all-optical packet switched cross connects," IEEE Photon. Lett., vol. 14, no. 6, pp. 849-851 (2002).

[3] K. Y. Song, M. G. Herraez, and L. Thevenaz, "Observation of pulse delaying and advancement in optical fibers using stimulated Brillouin scattering," Opt. Express, vol. 13, pp. 82 - 88 (2005).

[4] Y. Okawachi, M. S. Bigelow, J. E. Sharping, Z. Zhu, A. Schweinsberg, D. J. Gauthier, R. W. Boyd, and A. L. Gaeta, "Tunable all-optical delays via Brillouin slow light in an optical fiber," Phys. Rev. Lett., vol. 94, 15, 153902 (2005).

[5] Mable P. Fok and Chester Shu, "Tunable pulse delay using spectral filtering from a nonlinearly broadened optical spectrum and group velocity dispersion in a chirped fiber Bragg grating," in Proc. ECOC 07, P021.

[6] Mable P. Fok and Chester Shu, "Tunable optical delay usinf four-wave mixing in a 35-cm highly nonlinear bismuth-oxide fiber and group velocity dispersion," J. Lightw. Technol., vol. 26, no. 5, pp. 499-504 (2008).

[7] Y. Okawachi, J. E. Sharping, C. Xu, and A. L. Gaeta, "Large tunable optical delays via self-phase modulation and dispersion," Opt. Express, vol. 14, 12022-12027 (2006).

[8] S. Lee, S. Kim, B. Kang, and J. Park, "All-optical serial-to-parallel and parallel-to-serial data converters based on Mach-Zehnder interferometer," in Proc. of IEEE LEOS 2000, MM2.

[9] K. Vlachos, G. Theophilopoulos, A. Hatziefremidis, and H. Avramopoulos, "30 Gb/s all-optical clock recovery circuit," IEEE Photon. Technol. Lett., vol. 12, no. 6, pp. 705-707 (2000).

[10] K. L. Hall and K. A. Rauschenbach, "100 Gb/s bitwise logic," Opt. Lett., vol. 15, 1271-1273 (1998).

[11] T. Ohno, K. Sato, R. Iga, Y. Kondo, K. Yoshino, T. Furuta, and H. Ito, "Recovery of 80 GHz optical clock from 160 Gbit/s data using regeneratively modelocked laser diode," Electron. Lett., vol. 39, no. 19, pp. 1398-1400 (2003).

[12] K. P. Hansen, J. R. Folkenberg, C. Peucheret and A. Bjarklev, "Fully dispersion controlled triangular-core nonlinear photonic crystal fiber," in Proc. Optical Fiber Communication Conference 2003, PD2-1.

CHAPTER 6

Tunable optical delay with CSRZ-OOK to RZ-OOK optical data format conversion using four-wave mixing wavelength conversion and group velocity dispersion

---

In this chapter, an optically controlled tunable delay scheme with simultaneous CSRZ-OOK to RZ-OOK data format conversion has been proposed using pump-modulated four-wave mixing (FWM) wavelength conversion in a 64-m dispersion flattened nonlinear photonic crystal fiber (PCF) together with group velocity dispersion (GVD) in a chirped fiber Bragg grating (CFBG). By exploiting phase doubling on the input signal, CSRZ-OOK to RZ-OOK format and wavelength conversion is achieved. The dispersion flattened nonlinear PCF offers a conversion bandwidth of about 16 nm. With the use of a CFBG, a delay range over 200 ps has been experimentally demonstrated. The approach does not require any clock signal and is transparent to the bit rate. The system performance has been measured and no power penalty is introduced.

6.1 Introduction

Tunable optical delay line has attracted much research interest as a key component in optical communications. The delay is required for optical buffering or delaying of signal arrival during their processing at the bottleneck of an optical communication network. Different approaches have been experimentally demonstrated to realize an optical tunable delay. Examples of which are the recirculation of optical information in a fiber loop [1] and the switching of light to different optical propagation paths [2]. To achieve continuously tunable delay, slow light techniques attract much attention. The techniques are based on laser-induced resonance to reduce the group velocity [3]. Slow light can be achieved with electromagnetically induced transparency [4], coherent population oscillations [5], stimulated Brillouin scattering [6], and stimulated Raman scattering [7]. Apart from slow light techniques, tunable delay can be achieved with wavelength conversion together with group velocity dispersion [8][9][10]. To increase the speed and bandwidth efficiency of an optical communication system, much research has been conducted recently on the use of different modulation formats other than the traditional non-return-to-zero (NRZ) and return-to-zero (RZ). Carrier-suppressed return-to-zero (CSRZ) data format demonstrates certain advantages in 40-Gb/s communication system because of its tolerance to some of the nonlinearities in long haul fiber network [11]. However, to adopt CSRZ data format, a system must be optimized with different optical settings in dispersion and fiber nonlinearity management. Optical data format conversion is therefore desirable for future communication network employing different modulation formats. The all-optical approach has received much attention since all-optical signal processing offers a higher processing speed compared to traditional electrical-to-optical and

optical-to-electrical conversion. All-optical conversion between NRZ and RZ formats has been achieved with many different methods. Examples of which are spectral filtering from a cross-phase modulation output [12], the use of a nonlinear optical loop mirror [13], and the use of dual-wavelength injection locking [14]. The conversion between CSRZ and RZ formats can be achieved using a semiconductor optical amplifier (SOA) based fiber loop mirror [15] or a periodically poled lithium niobate (PPLN) device [16]. An optical clock or a carrier suppressed clock is required to modulate the phase of the signal to achieve format conversion.

To obtain tunable delay with CSRZ to RZ format conversion, we propose to use pump modulated four-wave-mixing (FWM) wavelength converter built by a highly nonlinear photonic crystal fiber (PCF) followed with group velocity dispersion provided by a chirped fiber Bragg grating. PCF-based pump modulated FWM has been previously applied for all-optical signal regeneration in on-off keying (OOK) [17] signal. The phase doubling characteristic has also used for extinction ratio enhancement in differential phase-shifted keying (DPSK) signal [18]. In this chapter, we demonstrate 10-Gb/s optical format conversion from CSRZ to RZ with continuously tunable delay. The conversion is based on the doubling of phase in the input signal. The output maintains the same phase in every bit, resulting in a RZ data signal. The bit-error-rate (BER) performance is measured experimentally. No optical clock or control signal is required in the process and the approach is thus transparent to the bit-rate. Because of the fast response of FWM in an optical fiber, the approach is potentially applicable for 40 Gb/s or even higher data rates.

6.2 Carrier-Suppressed Return-to-Zero

Carrier-Suppressed Return-to-Zero (CSRZ) is an optical signal format. Similar to conventional Return-to-Zero (RZ) modulation, the intensity drops to zero between consecutive bits. But field phase alternates by π between neighboring bits. CSRZ format can be generated by different methods, such as spectral filtering [19], biasing the Mach-Zehnder modulator (MZM) at null point and driven with sinusoidal signal [20]. CSRZ can be used to generate specific optical modulation formats, such as CSRZ-OOK, in which data is coded on the intensity of the signal using a binary scheme, or CSRZ-DPSK, in which data is coded on the differential phase of the signal. CSRZ-OOK signal is considered to be more tolerance to narrowband filtering, dispersion and fiber nonlinearity as described in [11]. The generation scheme of 10-Gb/s CSRZ-OOK using MZM is shown in figure. The CSRZ signal is generated by biasing the MZM at null point and is driven by a sinusoidal signal at 5 GHz. The output from the MZM is a 10-GHz CSRZ waveform. The 10-Gb/s data is added on this waveform via another stage of modulation to produce the CSRZ-OOK signal.

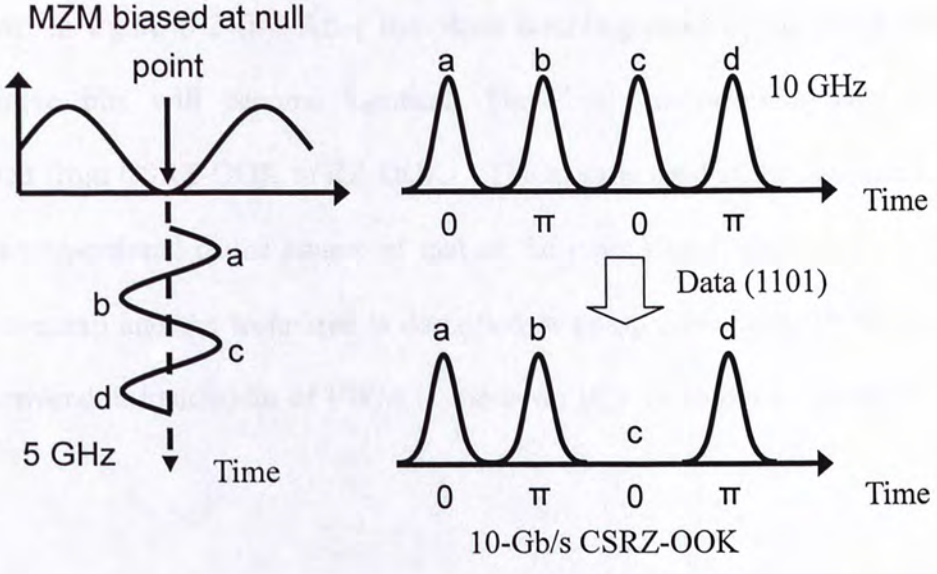

Figure 6-1: Schematic illustration of CSRZ-OOK generation

6.3 Operating Principle

Our tunable delay line is composed of two parts. The first part is a wavelength and data format converter using pump modulated FWM in a 64-m PCF. The conventional FWM was described in section 5.2. With a CW control light at ω_C and signal at ω_S, two new waves will be generated at $\omega_3 = 2\omega_C - \omega_S$ and $\omega_4 = 2\omega_S - \omega_C$ as shown in figure 6-2 (a). The new waves can be expressed as:

$$E_3 = (\vec{E}_C \cdot \vec{E}_S^{\,*}) E_C \gamma(\omega_C - \omega_S) \exp[i(\omega_3 t + 2\varphi_C - \varphi_S)] \qquad (6.1)$$

$$E_4 = (\vec{E}_S \cdot \vec{E}_C^{\,*}) E_S \gamma(\omega_S - \omega_C) \exp[i(\omega_4 t + 2\varphi_S - \varphi_C)] \qquad (6.2)$$

Note that the phase of the generated wave at ω_3 is $2\varphi_C - \varphi_S$. The phase information of the signal will be carried to the output at ω_3. The phase of another generated wave at ω_4 is $2\varphi_S - \varphi_C$. The phase of the signal is thus doubled. In our scheme, we use the phase doubling characteristic of pump-modulated FWM to achieve data format conversion. For CSRZ-OOK signal, the phase between consecutive bits differs by π as shown in figure 6-2 (b). After the phase doubling process, the phase between consecutive bits will become identical. Therefore, the incoming data will be converted from CSRZ-OOK to RZ-OOK. The electric field of the converted signal at ω_4 is proportional to the square of that of the input signal. Therefore, the signal acts at a pump and the technique is described as pump modulated FWM [21]. The 3-dB conversion bandwidth of FWM in the 64-m PCF is 16 nm as shown in figure 6-3.

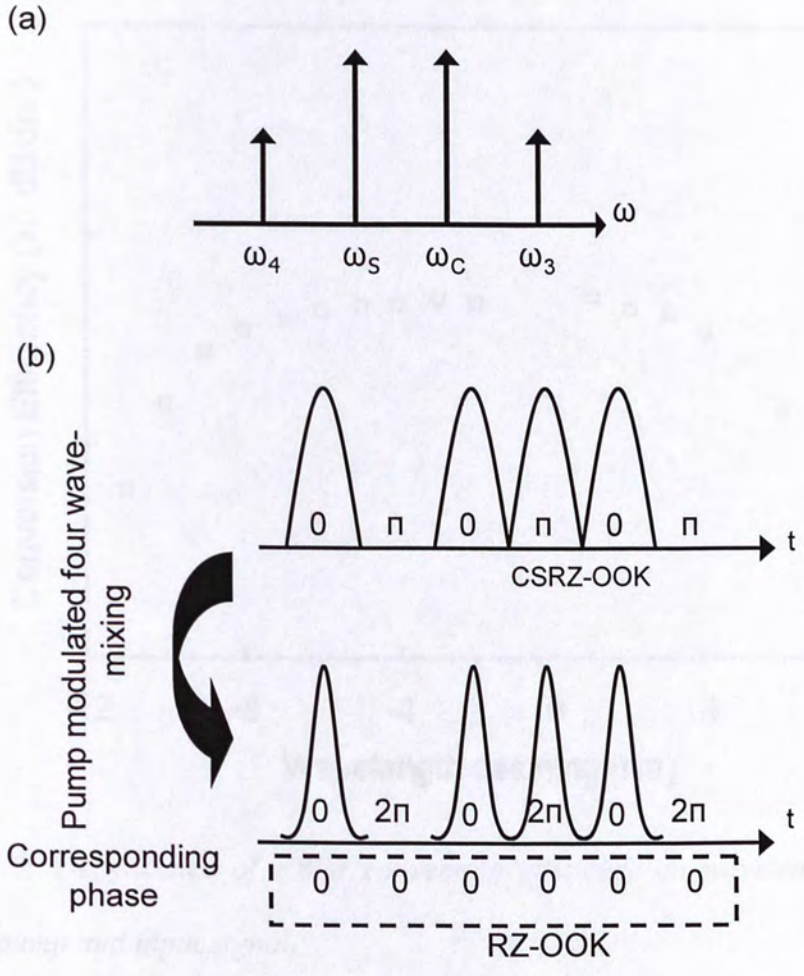

Figure 6-2: (a) Different spectral components in FWM. ω_C: input control frequency (CW); ω_S: input signal frequency; ω_3: conventional FWM output frequency; ω_4: pump-modulated FWM output frequency (b) Schematic illustration of CSRZ-OOK to RZ-OOK data format conversion via phase doubling effect in pump modulated FWM.

The second part introduces a wavelength dependent time delay using group velocity dispersion. The dispersion is introduced by a CFBG. Since different wavelengths are reflected at different positions in the CFBG, a wavelength dependent time delay is achieved. The change in the time delay is $\Delta t = D \cdot \Delta\lambda$, where D is the dispersion coefficient of the CFBG and $\Delta\lambda$ is the wavelength shift.

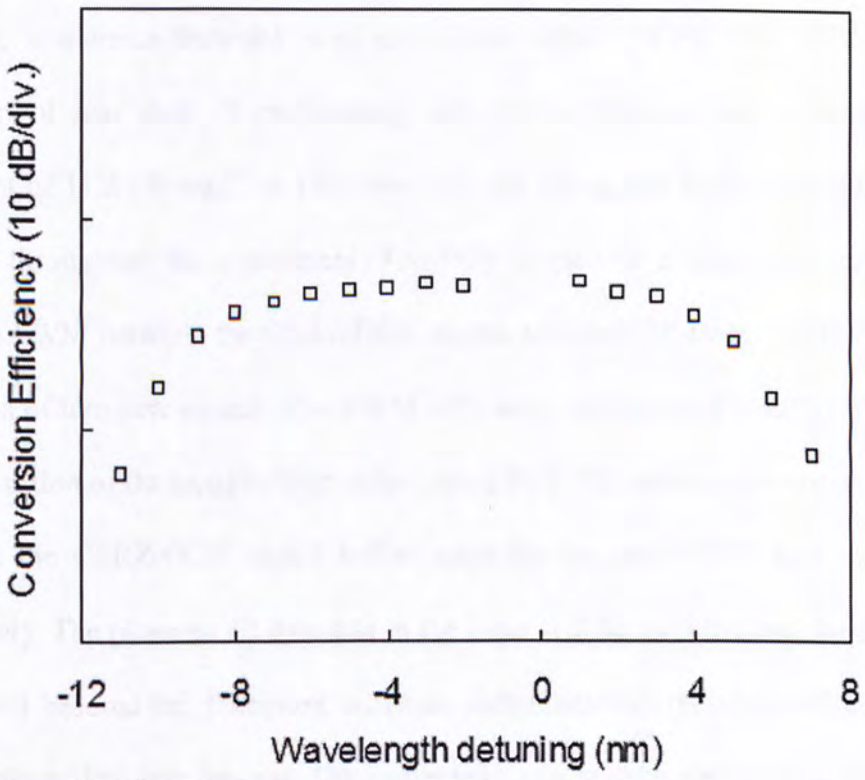

Figure 6-3: Dependence of FWM conversion efficiency on wavelength detuning between pump and input signal.

6.4 Experimental setup

Our setup is shown in figure 6-4. The signal is prepared by externally modulating a laser diode using an electro-optic intensity modulator (EOM) driven by a 5 GHz sinusoidal RF signal. The EOM is electrically biased at the transmission notch to produce a carrier-suppressed optical waveform at 10 GHz as shown in the inset of figure 6-4. The waveform is again modulated by another EOM driven by a pulse pattern generator at 10 Gb/s (2^{31}-1 PRBS) to produce a 10-Gb/s CSRZ-OOK signal. The polarization controllers (PC1 and PC2) are used to optimize the signal polarization for the modulations. A CW tunable laser is combined with the CSRZ-OOK signal via a 3-dB coupler. The combined output is amplified to produce

an average power of 20 dBm using an EDFA and is then directed to the 64-m highly nonlinear, dispersion-flattened photonic crystal fiber (PCF). The PCF has a dispersion of less than -3 ps/(km•nm) over 1500-1600 nm and a nonlinearity coefficient of 11.2 $(W•km)^{-1}$ at 1550 nm [10]. No stimulated Brillouin scattering is observed throughout the experiment. The PCF is used as a nonlinear medium to introduce FWM between the CSRZ-OOK signal and the CW laser, resulting in the generation of two new signals. The FWM efficiency can be maximized by adjusting the polarization of the tunable laser output using PC3. The average power of the CW light and the CSRZ-OOK signal before amplification are -17.65 and -22 dBm, respectively. The phase of all data bits in the input will be doubled and the phase of bit "π" will become 2π. Therefore, no phase difference will remain in adjacent bits after the phase doubling process. The converted signal will be converted to RZ-OOK. An optical tunable bandpass filter with a 0.4 nm 3-dB bandwidth is used to filter out the converted signal. The converted wavelength can be adjusted by changing the pump wavelength. To achieve tunable delay simultaneously, the converted signal is directed to a CFBG via an optical circulator. When the converted wavelength is changed, the converted signal will be reflected at different positions along the CFBG. The dispersion of the CFBG is 20 ps/nm. Thus a variable time delay can be obtained. The signal is then measured with a 36-GHz photo-detector and displayed by a sampling oscilloscope. The relative time delay is determined by measuring the waveform traces displayed on the oscilloscope. The quality of the converted RZ-OOK signal is analyzed using a 10-Gb/s bit-error-rate tester.

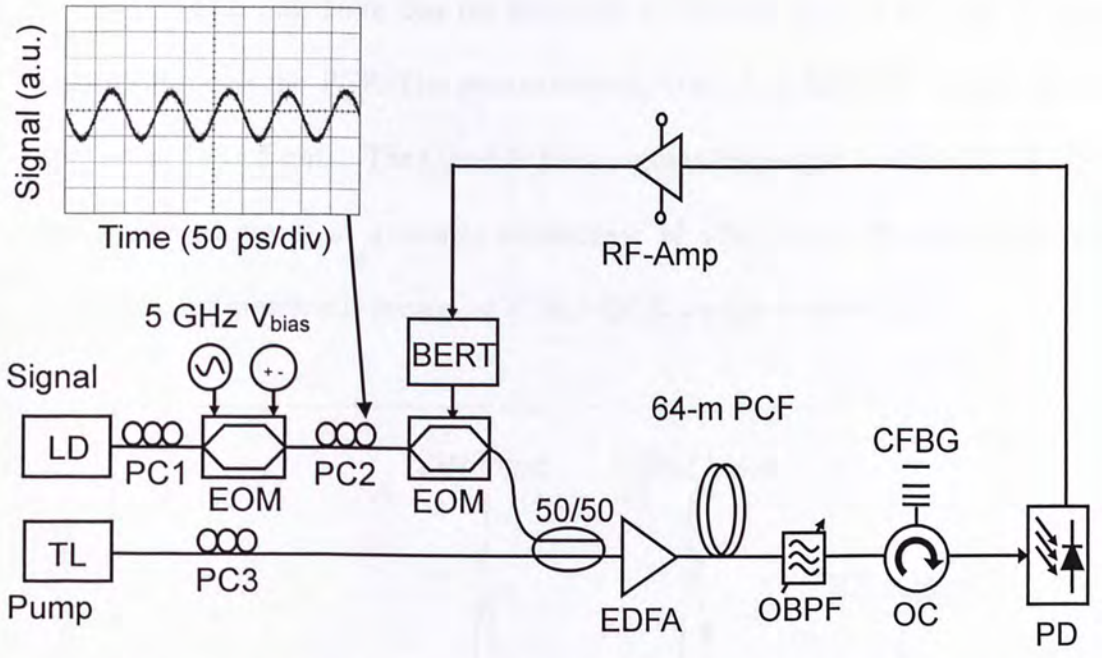

Figure 6-4: Experimental setup of the CSRZ-OOK to RZ-OOK all-optical data format converter. LD: laser diode; TL: tunable laser; PC: polarization controller; EOM: electro-optic intensity modulator; 50/50: 3-dB coupler; EDFA: erbium doped fiber amplifier; PCF: photonic crystal fiber; OBPF: optical bandpass filter; OC: optical circulator; CFBG: chirped fiber Bragg grating; PD: photo-detector; RF-Amp: radio frequency amplifier; BERT: bit-error-rate tester. Inset: carrier-suppressed waveform at 10 GHz

6.5 Experimental result

Figure 6-5 shows the optical spectra measured at different positions of the experimental setup. The optical spectrum analyzer has a resolution of 0.01 nm. The lower curve shows the spectrum of the signal and the CW tunable laser before they enter the PCF. The wavelength of the CW light and the signal are 1547.5 and 1549.5 nm, respectively. The upper curve depicts the spectrum measured after the PCF. FWM occurs in the PCF and two new signals are now generated at 1551.5

nm and 1545.5 nm. Note that the linewidth of the CW laser is broadened after passing through the PCF. The phase-doubled, converted RZ-OOK output signal appears at 1551.5 nm. The signal to noise ratio of the output is about 18 dB. For the generated signal at a shorter wavelength of 1545.5 nm, the phase and the amplitude information is preserved. CSRZ-OOK format is maintained.

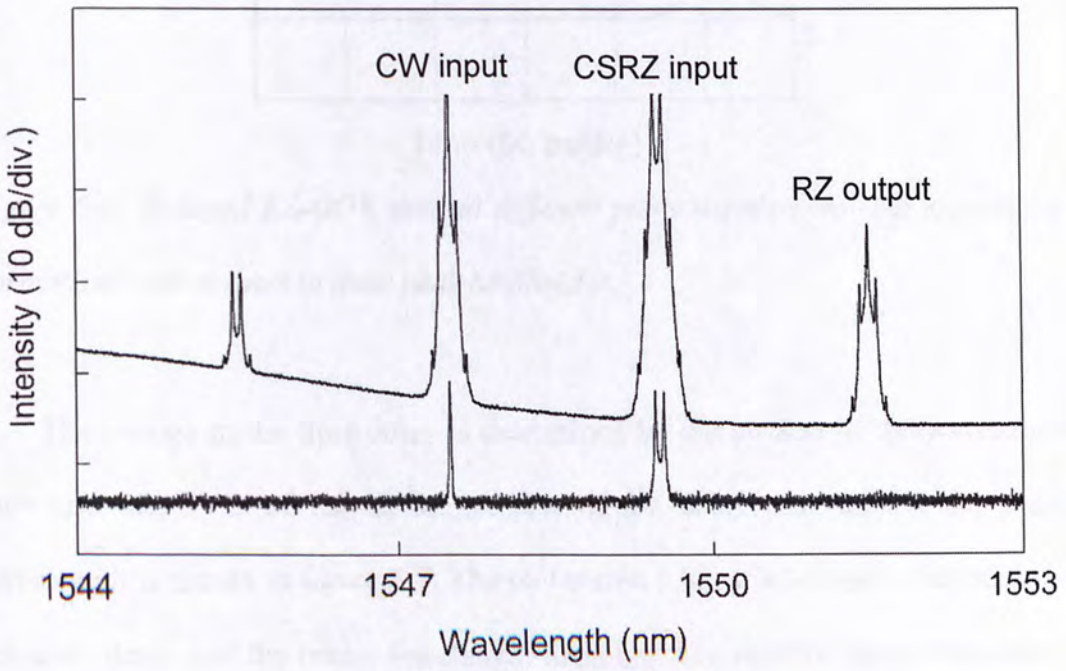

Fig. 6-5: Optical spectra measured at different positions of the experimental setup. Lower curve: optical spectrum obtained before the PCF. Upper curve: optical spectrum of the FWM output obtained after the PCF.

When the pump is tuned from 1547.5 to 1537.5 nm, the converted wavelength is changed from 1551.5 to 1561.5 nm. The converted output is directed to the CFBG and different wavelength are reflected at different positions along the grating. To estimate the delay achieved, the input CSRZ-OOK signal is set to be "1000000000". The delayed optical RZ-OOK signal profiles obtained at different pump wavelengths are displayed in figure 6-6.

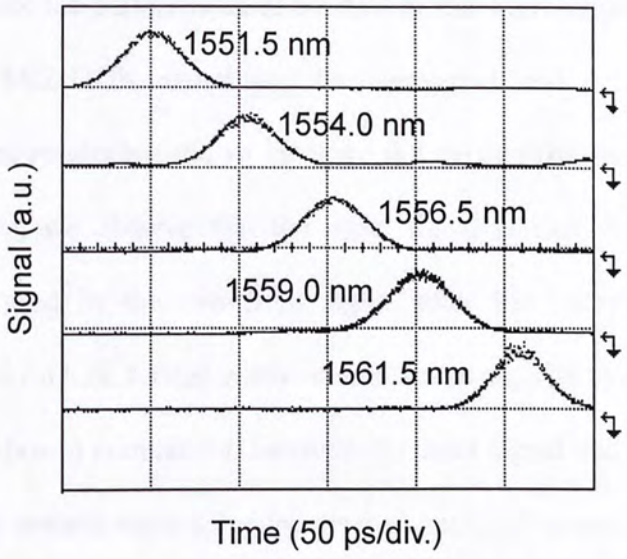

Figure 6-6: Delayed RZ-OOK data at different pump wavelengths. The signals are normalized with respect to their peak amplitudes.

The change in the time delay is determined by the product of the wavelength shift and the GVD of the CFBG. A plot of the delay time against the pump wavelength is shown in figure 6-7. The plot shows a linear relationship between the achieved delay and the pump wavelength detuning. The relative delay is measured with the reference of the converted signal at 1551.5 nm. The linear plot indicates that the dispersion is uniform across the reflection band.

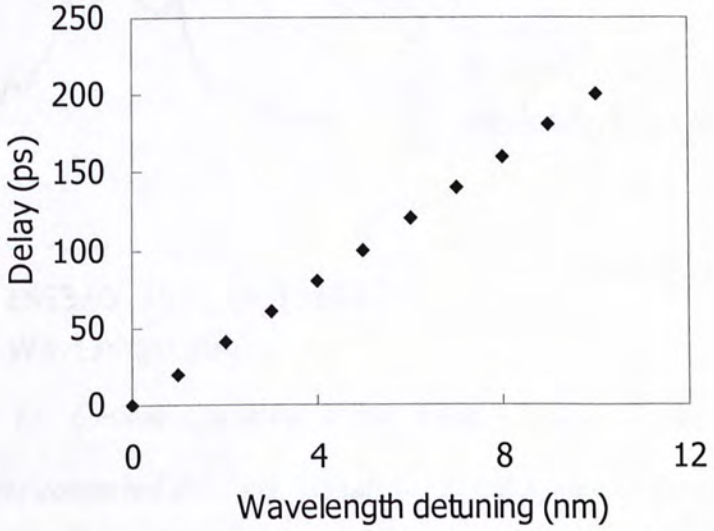

Figure 6-7: Plot of the time delay against the pump wavelength detuning

To investigate the performance of the data format conversion, the optical spectra of the input CSRZ-OOK signal and the converted and delayed RZ-OOK are measured and the results are shown in figure 6-8 (a) and (b), respectively. From the measured spectra, we observe that the input signal is carrier suppressed but the carrier is recovered in the converted signal after the pump modulated FWM. CSRZ-OOK to RZ-OOK format conversion is achieved. The eye-diagrams in figure 6-8 (c) and (d) show a comparison between the input signal and converted signal. A clear and widely opened eye is achieved for the converted output.

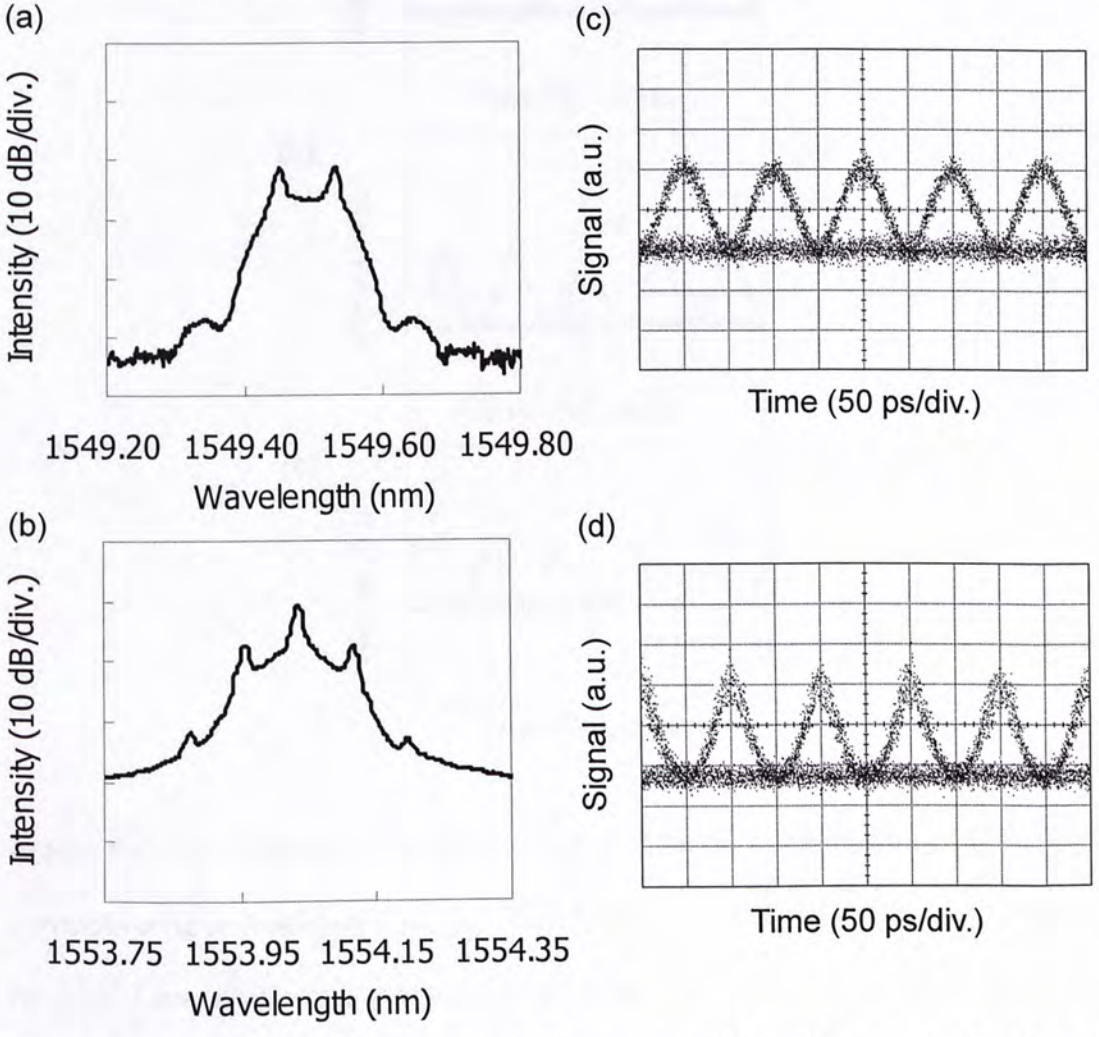

Figure 6-8: (a) Optical spectrum of the input CSRZ-OOK signal; (b) Optical spectrum of the converted RZ-OOK signal; (c) Eye diagram of the input CSRZ-OOK signal; (d) Eye diagram of the converted RZ-OOK signal.

Figure 6-9 shows the eye diagrams of the converted RZ-OOK signal at different delays. To investigate the performance of our system, a 10-Gb/s BER measurement is carried out. Figure 6-10 plots the output BER against the received optical power. The BER characteristics of the input CSRZ-OOK and the converted RZ-OOK signals are obtained.

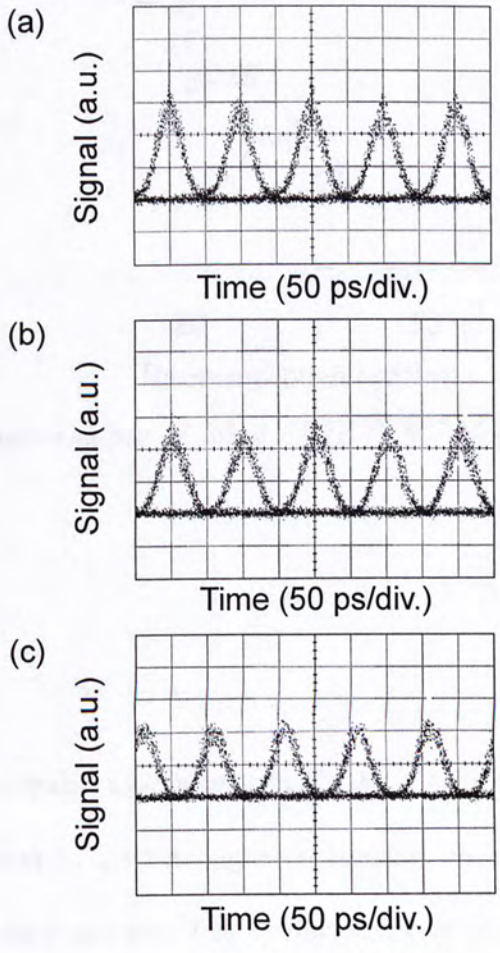

Figure 6-9: Eye diagrams of delayed signal at different wavelength. (a) 1551.5 nm corresponding to a delay of 0 ps; (b) 1556.5 nm corresponding to a delay of 140 ps; (c) 1561.5 nm corresponding to a delay of 200 ps.

Considering the BER at 10^{-9}, a power penalty of 0 to -1 dB is achieved for format converted outputs at different delays. The improvement is mainly attributed to

the shorter signal pulses that favor higher receiver sensitivity for RZ-OOK data format.

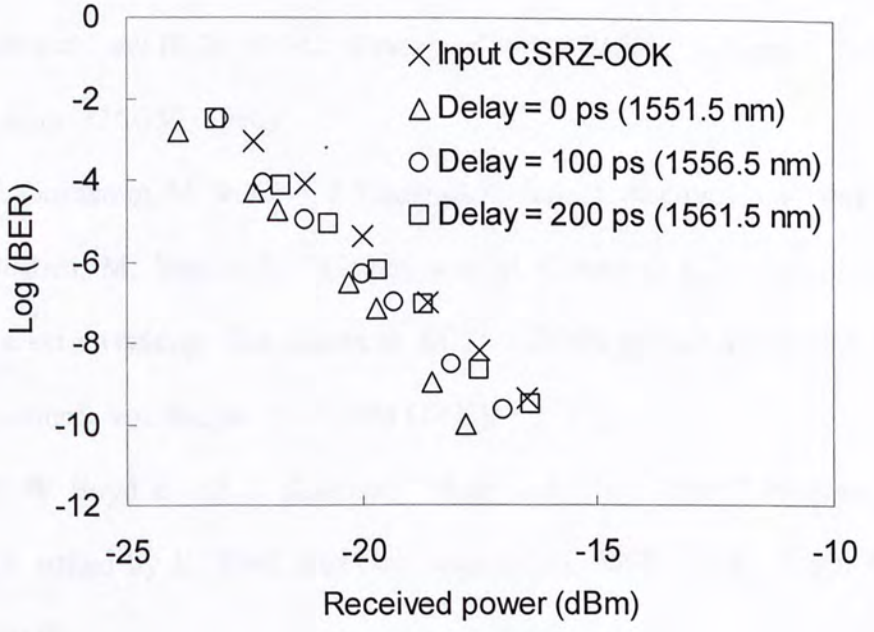

Figure 6-10: BER performance of input CSRZ-OOK signal and delayed RZ-OOK signals.

Conclusion

We have demonstrated all-optical tunable delay with CSRZ-OOK to RZ-OOK data format conversion in a 64-m highly nonlinear, dispersion flattened photonic crystal fiber. Using the phase doubling characteristic of pump modulated FWM and the group velocity dispersion in a CFBG, a bit-rate transparent optical delay line with CSRZ-OOK to RZ-OOK data format conversion is achieved. No optical clock is required to modulate the phase of the input signal. The maximum delay achieved is 200 ps. No degradation is incurred in the receiver sensitivity at a BER of 10^{-9}. The proposed setup offers a simple solution to delay and convert CSRZ data to RZ data in high speed optical communication network.

References

[1] R. Langenhorst, M. Eiselt, W. Pieper, G. Großkopf, R. Ludwig, L. Küller, E. Dietrich, and H. G. Weber, "Fiber loop optical buffer," J. Lightw. Technol., vol. 14, pp. 324-335 (1996).

[2] C. Guillemot, M. Renaud, P. Gambini, C. Janz, I. Andonovic, R. Bauknecht, B. Bostica, M. Burzio, F. Callegati, and M. Casoni et al., "Transparent optical packet switching: The European ACTS KEOPS project approach," J. Lightw. Technol., vol. 16, pp. 2117-2134 (1998).

[3] R. W. Boyd and D. J. Gauthier, "'Slow' and 'Fast' Light," *Progress in Optics* 43, edited by E. Wolf (Elsevier, Amsterdam, 2002), Chap. 6, pp. 497 – 530 (2002).

[4] M. M. Kash, V. A. Sautenkov, A. S. Zibrov, L. Hollberg, G. R.Welch, M. D. Lukin, Y. Rostovtsev, E. S. Fry, and M. O. Scully, "Ultraslow group velocity and enhanced nonlinear optical effects in a coherently driven hot atomic gas," Phys. Rev. Lett., vol. 82, pp. 5229–5232 (1999).

[5] M. S. Bigelow, N. N. Lepeshkin, and R. W. Boyd, "Observation of ultraslow light propagation in a ruby crystal at room temperature," Phys. Rev. Lett., vol. 90, no. 11, p. 113 903 (2003).

[6] Y. Okawachi, M. S. Bigelow, J. E. Sharping, Z. Zhu, A. Schweinsberg, D. J. Gauthier,R.W. Boyd, and A. L. Gaeta, "Tunable all-optical delays via Brillouin slow light in an optical fiber," Phys. Rev. Lett., vol. 94, p.153 902 (2005).

[7] J. E. Sharping, Y. Okawachi, and A. L. Gaeta, "Wide bandwidth slow light using a Raman fiber amplifier," Opt. Express, vol. 13, pp. 6092–6098 (2005).

[8] J. E. Sharping, Y. Okawachi, J. van Howe, C. Xu, Y. Wang, A. E. Willner, and A. L. Gaeta, "All-optical, wavelength and bandwidth preserving, pulse delay based on parametric wavelength conversion and dispersion," Opt. Express, vol. 13, pp. 7872–7877 (2005).

[9] S. Oda and A. Maruta, "All-optical tunable delay line based on soliton self-frequency shift and filtering broadened spectrum due to self-phase modulation," Opt. Express, vol. 14, pp. 7895–7902 (2006).

[10] Mable P. Fok and Chester Shu, "Tunable optical delay using four-wave mixing in a 35-cm highly nonlinear bismuth-oxide fiber and group velocity dispersion," J. Lightw. Technol., vol. 26, no. 5, pp. 499-504 (2008).

[11] A. Agarwal, S. Banerjee, D. F. Grosz, A. P. Küng, D. N. Maywar, A. Curevich, and T. H. Wood, "Ultra-high-capacity long-haul 40-Gb/s WDM transmission with 0.8-b/s/Hz spectral efficiency by means of strong optical filtering," IEEE Photon. Technol. Lett., vol. 15, pp. 470-472 (2003).

[12] S. H. Lee, K. K. Chow, and C. Shu, "Spectral filtering from a cross-phase modulated signal for RZ to NRZ format and wavelength conversion," Opt. Expess, vol. 13, pp. 1710-1715 (2005).

[13] L. Xu, B. C. Wang, V. Baby, I. Glesk, and P. R. Prucnal, "All-optical data format conversion between RZ and NRZ based on a Mach-Zehnder interferometric wavelength converter," IEEE Photon. Technol. Lett., vol. 15, pp. 308-310 (2003).

[14] C. W. Chow, C. S. Wong, and H. K. Tsang, "All-optical NRZ to RZ format and wavelength converter by dual-wavelength injection locking," Opt. Commun., vol. 209, pp.329-334 (2002).

[15] Wendi Li, Minghua Chen, Yi Dong, and Shizhong Xie, "All-optical format conversion from NRZ to CSRZ and between RZ and CSRZ using SOA-based fiber loop mirror," IEEE Photon. Technol. Lett., vol. 16, pp. 203-205 (2004).

[16] Jian Wang, Junqiang Sun, Xinliang Zhang, and Dexiu Huang "Proposal for PPLN-based all-optical NRZ-to-CSRZ, NRZ-DPSK-to-CSRZ-DPSK, and RZ-DPSK-to-CSRZ-DPSK format conversions," IEEE Photon. Technol. Lett., vol. 20, pp. 1039-1041 (2008).

[17] K. K. Chow, C. Shu, and Chinlon Lin, "Extinction ratio improvement by pump-modulated four-wave mixing in a dispersion flattened nonlinear photonic crystal fiber," Opt. Expess, vol. 13, pp. 8900-8905 (2005).

[18] M. P. Fok and Chester Shu, "DPSK signal extinction ratio enhancement using four-wave mixing in a highly nonlinear photonic crystal fiber," in Proc. Conference on Lasers and Electro-optics 2006, JThC63.

[19] Rongqing Hui, Benyuan Zhu, Renxiang Huang, Christopher T. Allen, Kenneth R. Demarest, and Douglas Richards, "Subcarrier Multiplexing for High-Speed Optical Transmission," J. Lightw. Technol., vol. 20, pp. 417-427 (2002).

[20] H. Schmuck, "Comparison of optical millimeter-wave system concepts with regard to chromatic dispersion," Electron. Lett., vol. 31, pp. 1848-1849 (1995).

[21] A. Bogris and D. Syvridis, "Regenerative properties of a pump-modulated four-wave mixing scheme in dispersion shifted fibers," J. Lightwave Technol., vol. 21, pp. 1892-1920 (2003).

CHAPTER 7

Conclusion

In this thesis, we have demonstrated different schemes to realize an all-optical tunable delay line. The all-optical tunable delay line enables the technology of optical packet switching technology which requires an optical buffer. The function of the tunable delay line is not limited to optical buffering. It can perform bit-synchronization in OTDM system, demodulation of DPSK signal, and etc.

7.1 Summary of work

In Chapter 2, we introduce the use of nonlinear polarization rotation (NPR) in a semiconductor optical amplifier (SOA) to perform switching of optical differential phase-shifted keying (DPSK) signal. A wavelength retaining 1 x 2 all-optical switch for DPSK signal has been constructed by commercial available components is presented. The switch can be used for implementing optical delay by switching the DPSK signal to different optical propagation paths. A 10-Gb/s NRZ-DPSK signal generated with 2^{31}-1 pseudorandom binary sequence (PRBS) is switched without changing its carrier wavelength. The switching utilizes NPR in an SOA. Using a polarization beam splitter (PBS), switching of DPSK signal between two output ports can be achieved. The phase information of the DPSK signal is preserved throughout the switching process. The performance of the switch is characterized using a 10-Gb/s bit-error-rate (BER) tester. The measured power penalty is below 3 dB over a 12-nm operating wavelength.

In Chapter 3, slow light via stimulated Brillouin scattering (SBS) using a phase modulated pump is proposed. The intrinsic Brillouin linewidth is restricted to approximately 30 MHz in conventional single mode fiber and therefore limits the useful data rate supported by SBS slow light system up to several tens of Mb/s. The phase modulated pump is proposed to enhance the bandwidth supported by slow light via SBS, hence supporting the delay of signal at telecommunication data rates (several Gb/s). Due to the constant intensity of the phase modulated pump, pump and signal synchronization is not required. A delay of 10 ps is achieved with a 26 ps optical pulse.

In Chapter 4, we demonstrate a wavelength transparent stimulated Brillouin scattering (SBS) approach for slow light. Our approach makes use of a cross gain modulation (XGM) based wavelength converter and a Brillouin fiber laser. The input signal is wavelength converted to become spectrally aligned to the resonance induced by SBS. The maximum delay achieved is 26 ns with a 30 dB Brillouin gain. The delay variation is less than 0.2 ns over 40-nm wavelength detuning of the input signal.

In Chapter 5, a channel selectable 40-Gb/s OTDM signal demultiplexing is demonstrated using an all-optical tunable delay line. The delay line is constructed using four-wave mixing (FWM) wavelength conversion together with group velocity dispersion (GVD). There is no inherent trade-off between the signal bandwidth and the amount of tunable delay. The demultiplexing is performed by optical gating in an electro-absorption modulator (EAM) via cross absorption modulation (XAM). By tuning the delay of the optical clock, fast channel selection can be achieved.

In Chapter 6, an optically controlled tunable delay scheme with simultaneous CSRZ-OOK to RZ-OOK data format conversion has been proposed using

pump-modulated four-wave mixing (FWM) wavelength conversion in a 64-m dispersion flattened nonlinear photonic crystal fiber (PCF) together with group velocity dispersion (GVD) in a chirped fiber Bragg grating (CFBG). By exploiting phase doubling on the input signal, CSRZ-OOK to RZ-OOK format and wavelength conversion is achieved. The dispersion flattened nonlinear PCF offers a conversion bandwidth of about 16 nm. With the use of a CFBG, a delay range over 200 ps has been experimentally demonstrated. The approach does not require any clock signal and is transparent to the bit rate.

7.2 Prospects of future work

To achieve the ultimate goal of all-optical buffering, the delay provided by slow light or tunable delay using wavelength conversion and chromatic dispersion is not sufficient. Fiber loop buffer and switching among different fiber delays offer long delay time or buffering time by simply increasing the length of the optical fiber. However, the achieved delay is only discretely tunable. A continuously tunable delay for optical buffering can be achieved by combining the advantages of both fiber loop and continuously tunable delay by either slow light or wavelength conversion with chromatic dispersion proposed in Chapter 3 and 5.

Wavelength independent operation and wideband signal support are desirable characteristics for an all-optical tunable delay line in a real communication system. The delay line can be constructed by applying either phase or intensity modulation on the pump in the wavelength transparent slow light approach as described in Chapter 4. By broadening the pump spectrum with modulation, the approach can be extended to support the delay of signal at 10 Gb/s. Hence a practical means to delay signal and true data can be realized in an optical communication system.

Another potential application of slow light techniques is in enhancing the efficiency of other nonlinear processes in an optical fiber. The slow light techniques increase the interaction time for other nonlinear processes and therefore enhance the efficiency. We propose to investigate the effect of SBS slow light on FWM in the same optical fiber. Since phase matching is required for FWM, the Brillouin pump which is counter propagating with the signal will not cause any interference to the FWM process.

Appendix: List of publications

I. Alan Cheng, M. P. Fok, and C. Shu, "Wideband SBS Slow Light in a Single Mode Fiber Using a Phase-Modulated Pump," 2007 OSA Conference on Lasers and Electro-Optics (CLEO 2007) organized by OSA/IEEE, paper JWA49/2, Baltimore, Maryland, USA, 2007.05.

II. Alan Cheng, M. P. Fok, and Chester Shu, "Wavelength-Retaining 1 x 2 Optical Router for DPSK Signal Using Nonlinear Polarization Rotation in a SOA," Optical Fiber Communication Conference and Exposition and the National Fiber Optic Engineering Conference (OFC/NFOEC 2008) OSA/IEEE Paper JTha40. San Diego, California, USA, 2008.02.

III. Alan Cheng, M. P. Fok, and Chester Shu, "Wavelength Transparent SBS Slow Light Using XGM-Wavelength Converter and Brillouin Fiber Laser," 2008 OSA Conference on Lasers and Electro-Optics (CLEO 2008) organized by OSA/IEEE, paper JWA33/2, San Jose, California, USA, 2008.05.

IV. M. P. Fok; Alan Cheng, and Chester Shu, "Slow Light in Optical Fibers using Stimulated Brillouin Scattering," the 5th International Conference on Optical Communications and Networks (ICOCN 2006) ,University of Electronic Science and Technology of Technology of China, pp. 237-240/4, Chengdu, China, 2006.09.

V. Lawrence R. Chen, Alan Cheng, Chester Shu, Serge Doucet, and Sophie LaRochelle, "Mode-Locked, Multi-Wavelength Erbium-Doped Fiber Laser with 25 GHz Spacing," 2007 OSA Conference on Lasers and Electro-Optics (CLEO 2007) organized by OSA/IEEE, paper CMC3/2, Baltimore, Maryland, USA, 2007.05.

VI. Lawrence R. Chen, Alan Cheng, Chester Shu, Serge Doucet, and Sophie LaRochelle, "46 x 2.5 GHz Mode-Locked Erbium-Doped Fiber Laser With 25-GHz Spacing," IEEE Photonics Technology Letters vol.19 no.23, pp.1871-1873. United States of America: IEEE LEOS, 2007.12.01.